2. MSC Optimally Require Their Original Milieu

Stem cells are indispensable entities in most multicellular organisms in that they are responsible for forming tissues during early development and for maintaining them in the adult stage. Because all somatic stem cells, including MSC, have the same genetic material, every cell type has the potential to express a stem cell phenotype under specific conditions; that is, tissue-specific flexibility is inherent. Mesenchymal cells, of which connective tissue is mainly composed, do not develop into a tissue or an organ. The cells synthesize the extracellular matrix by themselves and in vitro establish favorable environments for growth. Mesenchymal cell cultures can be made from suspensions of cells dissociated from tissues, and microscopical and biochemical analyses facilitate exploration of the effects of adding or removing specific molecules, such as hormones or growth factors.

Cells vary in their needs in a cell type–specific manner, and cells can therefore be categorized or defined by their requirements. Bone marrow–derived MSC, for example, can be compared with umbilical cord blood–derived MSC. Several methods are available for distinguishing between these two types of cells. One such method is flow cytometric analysis of markers that appear on the surfaces of the cells. Some surface marker characteristics of bone marrow–derived MSC are the same as those of cord blood–derived MSC (eg, $CD29^+$, $CD44^+$, $CD55^+$, $CD59^+$, $CD34^-$, and $CD117^-$ [10-12]). On the other hand, the CD90 and CD133 markers can be used to distinguish cord blood–derived cells from bone marrow–derived cells, because these markers are expressed in multipotent marrow-derived cells but not in cord blood–derived cells [12]. As yet, no surface markers have been identified that define MSC. Another method is complementary DNA microarray/chip technology. Because of the logical connection between gene expression and cell function, gene expression patterns can predict the variation in cell phenotypes and reveal novel phenotypic aspects of the cells and tissues studied. In mesenchymal cell culture, expression of genes encoding growth factor receptors is an important factor in microarray analysis–based investigations of the effects of growth factors, because cells dissociated from different tissues, such as bone marrow and cord blood, have different responses to growth factors (Table 1). This response affects differentiation potential. Bone marrow–derived cells can differentiate into osteoblasts, chondrocytes, cardiomyocytes, adipocytes, skeletal myocytes, and neural cells and do so according to the specific cell culture conditions, whereas cord blood–derived cells exhibit only osteogenic and adipogenic potential under the same conditions.

How can the microenvironment, culture conditions, or growth factors dictate the identity of MSC and their production of different progeny? Serum plays a critical role in the growth of cells in vitro by providing components such as amino acids, lipids, growth factors, vitamins, hormones, and attachment factors, by acting as a pH buffer, and by providing protease inhibitors. Most media for mesenchymal cell culture include a poorly defined mixture of macromolecules in the form of fetal calf serum; however, the use of serum for MSC culture makes it difficult to know which specific macromolecules a particular type of cell requires for survival and normal function. This difficulty led to the development of serum-free chemically defined media. In addition to the usual molecules, such specialized media will need to contain essential growth factors that the MSC require in culture. The primary requirements of MSC in culture reflect the origin of the cells; that is, investigators have to try to recreate the specific native tissue/organ milieu of the cells' origin. Identification of a means to create an "Elysium" or ideal stress-free native environments for cultivating and maintaining MSC will bestow significant benefits for future stem cell therapeutics.

3. The Paradox of Cell Growth versus Life Span

In cell culture it is important not only to remove animal serum from the culture medium (for reasons of medical safety with respect to infectious diseases [13-15]) but also to obtain large numbers of cells for use in therapy. Cells must be propagated in vitro to obtain the large numbers needed for biomedical procedures; however, Hayflick's problem is unavoidable in normal cells [16,17]. Most vertebrate cells stop dividing after a finite number of divisions in culture, a process called *senescence* [17,18]. Senescence is classified into two categories: "stress-induced premature senescence" (or "telomere-independent senescence") and "replicative senescence" (or "telomere-dependent senescence") [19-21]. Marrow-derived mesenchymal cells divide approximately 25 to 40 times [11,22] in culture before they cease dividing or reach senescence (M0, mortality stage 0, ie, premature senescence), whereas a few cells that overcome this step restart proliferation but stop dividing again in replicative senescence (M1) (Figure 1).

To resolve these problems, investigators can extend the life span of bone marrow–derived MSC via retroviral transduction of human telomerase reverse transcriptase (hTERT) and human papillomavirus type 16 E6 and/or E7 genes [11]. A significant observation is that an increase in telomerase

Table 1.
Reactivities of Mesenchymal Stem Cells to Growth Factors*

	MSC	UCB	UE6E7T-12	UE7T-13
PDGF	+++	+++	+++	+++
EGF	+++	++	+++	++
aFGF	+++	++	++	+
bFGF	+++	+++	+++	++
LIF	–	+	++	+
VEGF	+	+	+	–
HGF	–	–	+	–
IGF-1	+	+	–	–
IL-1	–	–	–	++
IL-6	–	–	+	–

*Plus and minus symbols show the strength of growth factor reactivity based on cell proliferation. MSC indicates human bone marrow–derived mesenchymal stem cells; UCB, human umbilical cord blood–derived mesenchymal stem cells; UE6E7T-12 and UE7T-13, MSC transduced with human papillomavirus type 16 E6 and/or E7, and human telomerase reverse transcriptase (hTERT); PDGF, platelet-derived growth factor; EGF, epidermal growth factor; aFGF, acidic fibroblast growth factor; bFGF, basic FGF; LIF, leukemia inhibitory factor; VEGF, vascular endothelial growth factor; IGF-1, insulin-like growth factor 1; IL-1, interleukin 1.

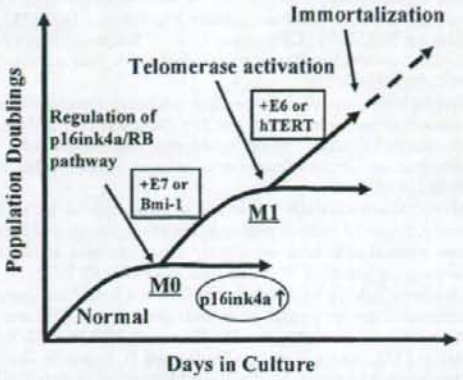

Figure 1. Life span of mesenchymal stem cells. Marrow-derived mesenchymal cells divide approximately 25 to 40 times in culture before they cease dividing or reach senescence (M0, mortality stage 0, ie, premature senescence). Some cells that overcome this step restart proliferation but stop dividing again in replicative senescence (M1). The system in which the p16ink4a/RB pathway is inhibited and telomerase is activated via transduction of *bmi-1*, human papillomavirus type 16 E6, E7, and hTERT is efficient in extending cellular life span.

activity produced via hTERT induction is insufficient to prolong the life span of bone marrow–derived MSC [23], because p16ink4a, a cyclin-dependent kinase inhibitor, is up-regulated [22]. This up-regulation of p16ink4a is directly linked to an increase in the number of cell doublings [24]. Inhibition of the p16/Rb pathway is sufficient to prolong the life span of cells in cultures of marrow-derived cells [11,22]. The p16ink4a/RB braking pathway leading to senescence can be inhibited by inducing the human papillomavirus type 16 E7 gene and/or *bmi-1*. *bmi-1*, one of the polycomb-group genes, has been used to inhibit p16ink4a transcription in order to prolong life span [25,26]. In addition, induction of the human papillomavirus type 16 E6 gene, which inhibits the p53 pathway, allows long-term cultivation of these cells. This system, in which the p16ink4a/RB pathway is inhibited and telomerase is activated, is highly efficient in extending the life span of bone marrow–derived MSC [23]. The life span of cord blood–derived MSC can be extended with hTERT alone [12].

Cell characteristics remain unaffected by *bmi-1*, E6, E7, and hTERT. The surface markers and the growth factor reactivities of transduced cells are unchanged (Table 1), and the transduced cells maintain their capabilities as stem cells [12,22]. So, can multipotent MSC with an extended life span be made available for cell-based therapy? It appears that transduced cells do not transform according to classic criteria: they do not generate a tumor in immunosuppressed interleukin 2 receptor knock-out NOD-SCID mice [22], they do not form foci in vitro, and they stop dividing after confluence. We cannot rule out the possibility, however, that gene-transduced bone marrow cells will become tumorigenic in patients several decades after commencement of cell therapy. What must be taken into account is that even when nononcogenic genes are introduced for cell-based therapy to increase cell growth and prolong life span, cases of leukemia have occurred in severe combined-immunodeficient patients treated with gene-modified lymphocytes [27]. Because of these failures, more time will be required before gene-modified cells can be used for regenerative medicine. Alleviation of culture stress is thus necessary to prolong the life span of mesenchymal cells.

Signaling from growth factor receptors caused by exogenously added growth factors induces p16ink4a protein through p38 and should selectively inhibit the prolongation of the cell life span without affecting growth factor–dependent cell proliferation through the classic Mek-Erk MAPK pathway (Figure 2A). Excessive stimulation by growth factors can be a cell senescence inducer, like oxidative stress and "culture shock" [28,29]. Growth factor–dependent acceleration of premature senescence or growth arrest is rather unexpected and unfavorable and is analogous to pressing down on the gas and brake pedals simultaneously [30,31]. Up-regulation of cell growth without affecting the cell life span, a key future goal of any cell-based therapy, would thus be a trade-off and create a fundamental quandary (Figures 2B and 2C).

4. Conclusion

Mammalian aging is associated with reduced regenerative capacity in tissues that contain stem cells. The aging process has been proposed to be at least partially caused by the senescence of progenitors with age; however, whether genes associated with senescence functionally contribute to physiological declines in progenitor activity has not yet been tested. Quantitative and qualitative changes do occur in stem cell populations with age [32-36]. The transition of multipotent stem cells to a more specific differentiated state is associated with simultaneous activation or inactivation of specific genes, and the promiscuous expression of many lineage-specific genes in primitive stem cells gradually decreases as cells reach a more mature state. Covalent modification

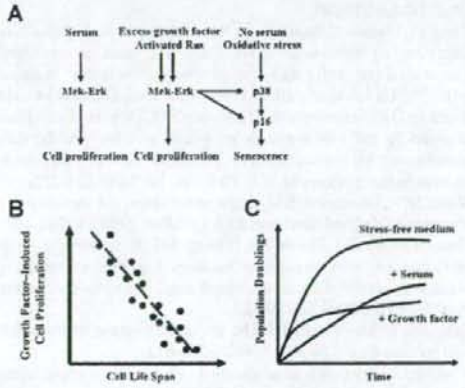

Figure 2. Signaling cascade and growth curves of mesenchymal stem cells for cell therapy. A, Scheme of the signaling cascade induced by stimuli leading to cell proliferation and senescence. B, Cell proliferation and the life span of mesenchymal cells are inversely correlated. C, Idealized cell growth profile in a stress-free medium. An ideal medium will help promote cell growth without affecting cellular aging.

includes acetylation, methylation, phosphorylation, and ubiquitination [37], and epigenetic regulation plays important roles in regulating gene expression. Consequently, the aging process influences stem cell–specific gene transcription. MicroRNA have recently been reported to be engaged in this regulation [38]. The goal of developing a clinically suitable medium for proliferating mesenchymal cells without affecting multipotency ex vivo appears feasible (Figure 2C), and its achievement should be beneficial to patients requiring an autologous or allogeneic transplant.

References

1. Alhadlaq A, Mao JJ. Mesenchymal stem cells: isolation and therapeutics. *Stem Cells Dev*. 2004;13:436-448.
2. Friedenstein AJ. Precursor cells of mechanocytes. *Int Rev Cytol*. 1976;47:327-359.
3. Makino S, Fukuda K, Miyoshi S, et al. Cardiomyocytes can be generated from marrow stromal cells in vitro. *J Clin Invest*. 1999;103:697-705.
4. Umezawa A, Maruyama T, Segawa K, Shadduck RK, Waheed A, Hata J. Multipotent marrow stromal cell line is able to induce hematopoiesis in vivo. *J Cell Physiol*. 1992;151:197-205.
5. Owen M. Marrow stromal stem cells. *J Cell Sci Suppl*. 1988;10:63-76.
6. Jaiswal N, Haynesworth SE, Caplan AI, Bruder SP. Osteogenic differentiation of purified, culture-expanded human mesenchymal stem cells in vitro. *J Cell Biochem*. 1997;64:295-312.
7. Pittenger MF, Mackay AM, Beck SC, et al. Multilineage potential of adult human mesenchymal stem cells. *Science*. 1999;284:143-147.
8. Sekiya I, Larson BL, Vuoristo JT, Cui JG, Prockop DJ. Adipogenic differentiation of human adult stem cells from bone marrow stroma (MSCs). *J Bone Miner Res*. 2004;19:256-264.
9. Horwitz EM. Mesenchymal cells: a basic review. 2002. Available at: http://www.celltherapysociety.org/files/documents/2005_Information_Booklet_-_Mesenchymal.doc. Accessed May 8, 2007.
10. Lee OK, Kuo TK, Chen WM, Lee KD, Hsieh SL, Chen TH. Isolation of multipotent mesenchymal stem cells from umbilical cord blood. *Blood*. 2004;103:1669-1675.
11. Takeda Y, Mori T, Imabayashi H, et al. Can the life span of human marrow stromal cells be prolonged by bmi-1, E6, E7, and/or telomerase without affecting cardiomyogenic differentiation? *J Gene Med*. 2004;6:833-845.
12. Terai M, Uyama T, Sugiki T, Li XK, Umezawa A, Kiyono T. Immortalization of human fetal cells: the life span of umbilical cord blood-derived cells can be prolonged without manipulating $p16^{INK4a}$/RB braking pathway. *Mol Biol Cell*. 2005;16:1491-1499.
13. Lennon DP, Haynesworth SE, Young RG, Dennis JE, Caplan AI. A chemically defined medium supports in vitro proliferation and maintains the osteochondral potential of rat marrow-derived mesenchymal stem cells. *Exp Cell Res*. 1995;219:211-222.
14. Wiles MV, Johansson BM. Embryonic stem cell development in a chemically defined medium. *Exp Cell Res*. 1999;247:241-248.
15. Yao CL, Chu IM, Hsieh TB, Hwang SM. A systematic strategy to optimize ex vivo expansion medium for human hematopoietic stem cells derived from umbilical cord blood mononuclear cells. *Exp Hematol*. 2004;32:720-727.
16. Hayflick L, Moorhead PS. The serial cultivation of human diploid cell strains. *Exp Cell Res*. 1961;25:585-621.
17. Campisi J. From cells to organisms: can we learn about aging from cells in culture? *Exp Gerontol*. 2001;36:607-618.
18. Wei W, Sedivy JM. Differentiation between senescence (M1) and crisis (M2) in human fibroblast cultures. *Exp Cell Res*. 1999;253:519-522.
19. Allsopp RC, Vaziri H, Patterson C, et al. Telomere length predicts replicative capacity of human fibroblasts. *Proc Natl Acad Sci U S A*. 1992;89:10114-10118.
20. Wright WE, Shay JW. The two-stage mechanism controlling cellular senescence and immortalization. *Exp Gerontol*. 1992;27:383-389.
21. Bodnar AG, Ouellette M, Frolkis M, et al. Extension of life-span by introduction of telomerase into normal human cells. *Science*. 1998;279:349-352.
22. Mori T, Kiyono T, Imabayashi H, et al. Combination of hTERT and *bmi-1*, E6, or E7 induces prolongation of the life span of bone marrow stromal cells from an elderly donor without affecting their neurogenic potential. *Mol Cell Biol*. 2005;25:5183-5195.
23. Okamoto T, Aoyama T, Nakayama T, et al. Clonal heterogeneity in differentiation potential of immortalized human mesenchymal stem cells. *Biochem Biophys Res Commun*. 2002;295:354-361.
24. Alcorta DA, Xiong Y, Phelps D, Hannon G, Beach D, Barrett JC. Involvement of the cyclin-dependent kinase inhibitor p16 (INK4a) in replicative senescence of normal human fibroblasts. *Proc Natl Acad Sci U S A*. 1996;93:13742-13747.
25. Haga K, Ohno S, Yugawa T, et al. Efficient immortalization of primary human cells by $p16^{INK4a}$-specific short hairpin RNA or Bmi-1, combined with introduction of hTERT. *Cancer Sci*. 2007;98:147-154.
26. Kim RH, Kang MK, Shin KH, et al. Bmi-1 cooperates with human papillomavirus type 16 E6 to immortalize normal human oral keratinocytes. *Exp Cell Res*. 2007;313:462-472.
27. Hacein-Bey-Abina S, Von Kalle C, Schmidt M, et al. LMO2-associated clonal T cell proliferation in two patients after gene therapy for SCID-X1. *Science*. 2003;302:415-419.
28. Sherr CJ, DePinho RA. Cellular senescence: mitotic clock or culture shock? *Cell*. 2000;102:407-410.
29. Toussaint O, Medrano EE, von Zglinicki T. Cellular and molecular mechanisms of stress-induced premature senescence (SIPS) of human diploid fibroblasts and melanocytes. *Exp Gerontol*. 2000;35:927-945.
30. Ramirez RD, Morales CP, Herbert BS, et al. Putative telomere-independent mechanisms of replicative aging reflect inadequate growth conditions. *Genes Dev*. 2001;15:398-403.
31. Raucci A, Laplantine E, Mansukhani A, Basilico C. Activation of the ERK1/2 and p38 mitogen-activated protein kinase pathways mediates fibroblast growth factor-induced growth arrest of chondrocytes. *J Biol Chem*. 2004;279:1747-1756.
32. Morrison SJ, Wandycz AM, Akashi K, Globerson A, Weissman IL. The aging of hematopoietic stem cells. *Nat Med*. 1996;2:1011-1016.
33. Harrison DE, Zhong RK, Jordan CT, Lemischka IR, Astle CM. Relative to adult marrow, fetal liver repopulates nearly five times more effectively long-term than short-term. *Exp Hematol*. 1997;25:293-297.
34. Kim M, Moon HB, Spangrude GJ. Major age-related changes of mouse hematopoietic stem/progenitor cells. *Ann N Y Acad Sci*. 2003;996:195-208.
35. Henckaerts E, Langer JC, Snoeck HW. Quantitative genetic variation in the hematopoietic stem cell and progenitor cell compartment and in lifespan are closely linked at multiple loci in BXD recombinant inbred mice. *Blood*. 2004;104:374-379.
36. Liang Y, Van Zant G, Szilvassy SJ. Effects of aging on the homing and engraftment of murine hematopoietic stem and progenitor cells. *Blood*. 2005;106:1479-1487.
37. Bandyopadhyay D, Medrano EE. The emerging role of epigenetics in cellular and organismal aging. *Exp Gerontol*. 2003;38:1299-1307.
38. Oakley EJ, Van Zant G. Unraveling the complex regulation of stem cells: implications for aging and cancer. *Leukemia*. 2007;21:612-621.

Glycoconj J (2008) 25:495–501
DOI 10.1007/s10719-007-9083-7

SHORT COMMUNICATION

The detergent-insoluble microdomains, rafts, can be used as an effective immunogen

Yohko U. Katagiri · Hideki Nakajima · Ban Sato · Yoshitaka Miyagawa · Yasuomi Horiuchi · Hajime Okita · Junichiro Fujimoto · Nobutaka Kiyokawa

Received: 17 May 2007 / Revised: 8 October 2007 / Accepted: 24 October 2007 / Published online: 11 December 2007

Abstract Detergent-insoluble microdomains, or rafts, act as a platform to transduce signals from the extracellular space into the cytoplasm. In the process of developing monoclonal antibodies against raft molecules for the purpose of studying the molecular mechanism of raft-mediated signaling, we observed the uniqueness and certain advantages of immunization with rafts. Simple subcutaneous injection of mice with a phosphate-buffered saline (PBS) suspension of rafts without mixing with Freund's adjuvant made it possible to increase the titer of antiserum reacting with raft components. Interestingly, injection of rafts prepared from certain specific cell lines induced monoglycolipid-specific antibodies. Furthermore, antibodies were produced by raft-immunization of even syngeneic mice. Our findings suggest that this phenomenon does not represent a breakdown of immunological self-tolerance, but typical immune reactions accompanying the class switch from IgM antibodies to IgG antibodies.

Keywords Raft · Antibody · Immune Response · Monoglycolipid-specific · Syngeneic antigen

Y. U. Katagiri (✉) · H. Nakajima · B. Sato · Y. Miyagawa · Y. Horiuchi · H. Okita · J. Fujimoto · N. Kiyokawa
Department of Developmental Biology, National Research Institute for Child Health and Development,
2-10-1 Okura, Setagaya-ku,
Tokyo 157-8535, Japan
e-mail: kata@nch.go.jp

Y. U. Katagiri · H. Okita · J. Fujimoto · N. Kiyokawa
CREST, Japan Science and Technology Corporation,
4-1-8 Honcho, Kawaguchi, Saitama 332-0012, Japan

Introduction

There is evidence that detergent-insoluble microdomains, or rafts, are important in signal transduction, because a variety of signaling molecules, such as Src-family kinases, heterotrimeric G proteins, and GPI-anchored proteins, are concentrated in rafts. We have previously shown that the binding of Shiga-toxin (Stx) to the globotriaosylceramide (Gb3[1]) in rafts temporally activates the Src-family kinase Yes in human renal cancer cell line ACHN [1]. In order to study the downstream signaling mechanism after Stx binding to Gb3, we attempted to develop monoclonal antibodies against components of rafts prepared from ACHN cells and established several clones [2].

In the process we observed the uniqueness of immunization using raft suspensions. Before immunizing animals in an attempt to induce antibody production, antigen solutions or cell suspensions are generally mixed with Freund's adjuvant to obtain an oil emulsion, whereas we succeeded in raising antibody titer by the raft immunization method without mixing them with adjuvants. Interestingly, two thirds of the clones obtained reacted with lipid components of the raft, and further analysis showed that all of the lipid-reactive clones recognized monosialosylgalactosylgloboside (sialylGb5).

To ascertain whether raft immunization always induces monospecific antibodies that recognize a certain glycolipid, we immunized mice with rafts prepared from several cell lines and examined the glycolipid antigens recognized by the antibodies induced. In this paper we report that injection with

[1] Glycosphingolipids are abbreviated according to the recommendation of the IUPAC-IUB Commission on Biochemical Nomenclature. http://www.chem.qmul.ac.uk/iupac/misc/glylp.html.

rafts prepared from certain specific cell lines can induce the production of monoglycolipid-specific antibodies and that raft immunization can induce antibody production even in syngeneic mice.

Materials and methods

Cell culture and antibodies Human renal cancer cell line ACHN, human T-cell leukemia cell lines Jurkat and MOLT-4, and mouse myeloma cell line P3U1 were purchased from the American Type Culture Collection, and the African green monkey kidney cell line Vero was a gift of Dr. T. Takeda of the Department of Infectious Diseases Research, National Children's Medical Research Center, Tokyo, Japan. Anaplastic large cell lymphoma Karpas 299 cells [3] were gifted by Dr. K. Kikuchi of Sapporo Medical University, School of Medicine, Sapporo, Japan. Human pre-B ALL cell line NALM-6, mouse T lymphoma cell line EL4, mouse melanoma cell line B16F1, and mouse leukemia cell line RL2 were obtained from the Institute of Development, Aging and Cancer of Tohoku University, Sendai, Japan. The ACHN cells, Vero cells, and B16F1 cells were cultured in Dulbecco's modified Eagle's medium (Sigma Chem., St. Louis, MO) supplemented with 10% fetal bovine serum (FBS) (Cansera International Inc., CCT, Canada). All other cell lines were cultured in RPMI 1640 supplemented with 10% FBS. The NZB/WF1 serum was a kind gift of Dr. S. Kon of the Institute of Genetic Medicine, Hokkaido University, Sapporo.

Raft preparation Rafts were prepared as described previously [2]. Briefly, packed cells were homogenized in 1% Triton lysis buffer (1% Triton X-100, 25 mM Tris–HCl buffer, pH 7.5, 0.15 M NaCl) by 20 strokes with a hand-driven Teflon glass homogenizer. Cell lysates, sucrose concentration of which was adjusted to 40% with 85% sucrose solution, were placed on the bottom of an ultracentrifuge tube, and a 5/30% discontinuous sucrose gradient was formed over the sample. After centrifugation at 39,000 rpm for 18 h at 4°C in a Beckman SW 40Ti rotor, rafts were recovered as visible bands at the interface between 5 and 30% sucrose solution. After several washes with PBS, raft suspensions in PBS were stored at −30°C until used.

Immunization of mice Rafts prepared from 1.2×10^6~1.5×10^8 cells or 10^7 cells irradiated at 10 Gy were suspended in 100 μl of PBS. They were subcutaneously injected into mice in triplicate, followed by three booster shots at 1-week intervals. Five days after the final injection, a peripheral blood specimen was collected from the mice, and the level of antibodies against rafts was evaluated.

TLC immunostaining Lipids were prepared from packed cells as previously described [4] and separated on a Silica gel 60-precoated HPTLC aluminium sheet (Merck, Darmstadt, Germany) with a solvent system consisting of chloroform/methanol/water containing 0.2% $CaCl_2$ (5:4:1, *v/v*). After drying, the TLC plates were coated with 0.1% polyisobutylmethacrylate (Sigma-Aldrich, Milwaukee, WI) in cyclohexane and blocked with 1% bovine serum albumin (BSA) in PBS. The plates were probed with anti-sera (diluted to 1:500 in 1% BSA in PBS) for 1 h at room temperature. After three washes with PBS for 5 min each, horseradish peroxidase (HRP)-conjugated rabbit anti-mouse immunoglobulins G+M (DAKO, A/S, Denmark) at a 1:2,000 dilution ratio were used as the second antibody. The antibodies that bound to the plates were visualized with enhanced chemiluminescence reagent Super Signal (Pierce, Rockford, IL) and detected with a luminescent imaging analyzer, LAS-1000 (Fuji Film, Tokyo, Japan). To compare the amounts of antibodies in the sera, the intensity of chemiluminescence was measured with Image Gauge analysis software equipped to LAS-1000 and shown as Photo Stimulated Luminescence (PSL).

Dot-blot immunostaining assay The ACHN rafts were dot-blotted on a PVDF membrane (Millipore Corp., Bedford, MA) and immunostained as described previously [2] with a slight modification. The dots were probed with antisera (diluted to 1 in 500 with 1% BSA in PBS) for 1 h at room temperature. After four washes with PBS containing 0.025% Tween 20 (PBS-Tween), the membranes were treated with HRP-conjugated rabbit anti-mouse IgG antibodies specific to Fcγ fragment and HRP-conjugated goat anti-mouse IgM antibodies specific to μ chain (Jackson Immuno Research Laboratories, West Grove, PA) to detect IgG and IgM, respectively. The antibodies that bound to the membrane were visualized with enhanced chemiluminescence (ECL Western blotting system; Amersham Pharmacia Biotech. UK Ltd., Buckinghamshire) and detected by a luminescent imaging analyzer as mentioned above.

Flow cytometry Cells were harvested from culture plates, and after incubating with the antisera (diluted to 1:100 in RPMI medium containing 5% FBS and 0.1% NaN_3) for 1 h on ice, they were treated with fluorescein isothiocyanate-conjugated goat anti-mouse immunoglobulins (Jackson Immuno Research Laboratories) at a 1:50 dilution ratio and analyzed by flow cytometry (EPICS-XL, Beckman-Coulter, Fullerton, CA).

Measurement of anti-ss and -dsDNA antibodies in sera by ELISA The ELISA was performed as described by Iizuka *et al.* [5] with a slight modification by using calf thymus ssDNA (Sigma) and salmon sperm dsDNA (Sigma). For

the substrate solution, 120 µl of 0.1 mg/ml 3,3′,5,5′-tetramethylbenzidine (Dojindo, Kumamoto, Japan) solution in *N,N*,dimethylformamide and 1.3 µl of 30% H_2O_2 was mixed with 7.88 ml of 0.1 M sodium acetate buffer, pH 5.5, immediately before use. A 0.5 µg amount of ssDNA or dsDNA dissolved in 50 µl of PBS were allowed to dry in a flat 96-well NUNC-IMMUNO Plate (Nunc, Roskilde, Denmark). Wells were blocked with 3% BSA in PBS and washed with PBS-Tween. A 50 µl of the serum (diluted to 1:100) was added to a well in triplicate, and allowed to stand at room temperature for 2 h. After five washes with PBS-Tween, HRP-conjugated donkey anti-mouse µ chain antibodies or rabbit anti-mouse γ chain antibodies (Jackson Laboratory; diluted to 1:2,000) in 1% BSA in PBS was added to each well and incubated for 1 h at room temperature. After three washes with PBS-Tween, 50 µl of substrate solution was added, and the plates were incubated at room temperature until the solution turned yellow. The reaction was stopped by adding 50 µl of 2 M H_2SO_4, and absorbance at 450 nm was measured with a microplate reader (Model 550 Bio-Rad, Richmond, CA).

Results and discussion

The antisera obtained from Balb/c mice in response to subcutaneous injection of rafts prepared from a variety of cell lines were examined by TLC-immunostaining to analyze the reactivity of the antibodies against glycolipids. Both ACHN cells and Vero cells are derived from kidney and express globoseries glycosphingolipids, whereas Karpas cells predominantly express LacCer, and EL4 cells mainly express GM2 and GD2 (Fig. 1a). The antisera obtained by injection with ACHN rafts and Vero rafts were found to uniquely bound to sialylGb5, suggesting the development of mono-specific antibodies against sialylGb5 (Fig. 1b). As we previously showed, ACHN cells contain comparable amounts of Gb3, Gb4, Gb5, and sialyGb5, suggesting that the sialylGb5 of ACHN cells is strongly immunogenic [2]. The antisera obtained by injection with Karpas rafts were also found to specifically bind to a single glycolipid that has not yet been identified. Since the glycolipid was stained with resorcinol and not bound by choleratoxin even after digestion with *Clostridium perfringens* sialidase (data not shown), it is suggested that this antigen is a sialylated non-ganglioseries glycolipid. The observation that the anti-Karpas rafts antisera did not bind to any glycolipid extracted from mouse brains in which various kinds of gangliosides are abundantly contained (data not shown) should support this idea. The antisera obtained by injection with EL4 rafts were found to uniquely react with GD2. However, when antisera obtained by injection of rafts prepared from the other cell lines, *i.e.*, B16F1, P3U1, RL-2, Molt 4, Jurkat, or NALM-6, were tested, no such monoglycolipid-specific reactivity was observed (data not shown). These findings indicate that immunization with rafts prepared from some specific cell lines can induce the development of monoglycolipid-specific antibodies. Since we obtained identical results in a similar experiment in C57BL/6 mice (Fig. 1c), the development of monoglycolipid-specific antibodies is a common feature of immunization of these cell lines with rafts and not a phenomenon specific to a certain strain of mice.

Immunization of mice with a suspension of whole cells is one of the ways that is often used to obtain monoclonal antibodies against cell surface molecules [6, 7]. We therefore investigated whether whole-cell immunization is capable of inducing the development of monoglycolipid-specific antibodies in mice, the same as raft immunization does. The antisera obtained by injection with Vero, Karpas, and EL4 cell suspensions did not react with certain specific glycolipids, and only the antisera obtained by immunization with ACHN cell suspensions yielded a mono-specific reaction with sialylGb5 (Fig. 2). This suggests that immunization with suspensions of whole cells does not usually induce the development of monoglycolipid-specific antibodies and that the rafts on the cell surface of ACHN cells assemble in a manner that is favorable for inducing immune reactions against sialylGb5.

Next, we examined the quantitative and qualitative kinetics of the production of the specific antibodies in sera by immunization with rafts derived from ACHN cells. The antisera obtained after each immunization were examined by dot-blot immunostaining and TLC immunostaining (Fig. 3a). The relative amounts of antibodies that bound to rafts dot-blotted on a PVDF membrane or lipids separated on a TLC plate were shown as PSL (Fig. 3b). Production of IgM class anti-raft antibodies was detected after the second immunization, and it peaked after the third immunization, and then decreased. Production of IgG class anti-raft antibodies was also detected after the second immunization, but at a low level, and it continued to increase even after the fourth immunization. The specificity of the secondary antibodies used for typing the immunoglobulin class of anti-raft antibodies was confirmed in advance (data not shown). No anti-sialylGb5 antibodies were detected not after the first immunization (data not shown). They were faintly detected after the second immunization, and then increased in an immunization time-dependent manner. These results indicate that the production of anti-raft antibodies in mice is a typical immune response accompanying the class switch from IgM antibodies to IgG antibodies. Interestingly, the #3 antisera of the third immunization gave strong reactivity with the lower band glycolipid, while that of the fourth

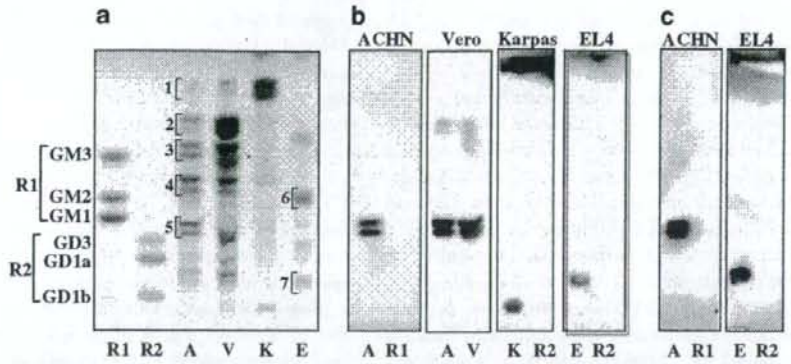

Fig. 1 TLC immunostaining with antisera against rafts components. The lipids extracted from ACHN (*A*), Vero (*V*), Karpas (*K*), EL4 (*E*) cells and the reference glycolipids (*R1* GM3, GM2, GM1; *R2* GD3, GD1a, GD1b) were separated by TLC and chemically stained with Orcinol reagent (**a**) or immunostained with antisera of Balb/c mice (**b**) and C57BL/6 mice (**c**) that had been immunized with rafts prepared from ACHN cells, Vero cells, Karpas cells and EL4 cells. Lipids extracted from 5×10^6 cells and 1×10^6 cells of each cell line are subjected to TLC for Orcinol staining and immunostaining, respectively. *1* LacCer; *2* Gb3; *3* Gb4; *4* Gb5; *5* sialylGb5; *6* GM2; *7* GD2

immunization reacted strongly with the upper band glycolipid (Fig. 3a). The result may indicate that ceramide structure is also involved in antigen presentation of glycolipid in rafts.

Next, we examined the correlation between the amounts of rafts injected and anti-raft antibody production. To do so, we immunized C57BL/6 mice with rafts prepared from various numbers of EL4 cells and evaluated the subsequent production of anti-EL4 raft antibodies by flow cytometry and TLC immunostaining. As shown in Fig. 4a, the amounts of anti-EL4 raft antibody increased with the amounts of EL4 rafts injected. Injection with the rafts prepared from 0.12×10^7 EL4 cells induced a slight elevation of reactivity, and the rafts prepared from 3×10^7 EL4 cells were sufficient to induce maximum reactivity. Rafts prepared from more than 0.6×10^7 EL4 cells appeared to be needed to obtain a significant level of anti-GD2 antibodies, (Fig. 4b).

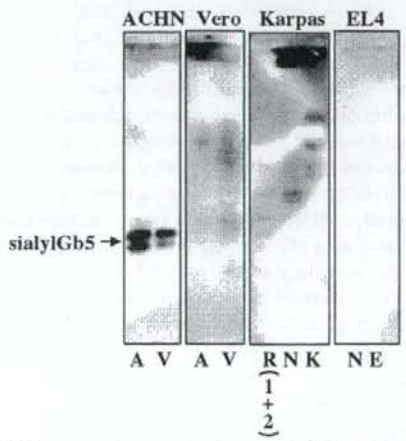

Fig. 2 TLC immunostaining with antisera against the cell suspension. The lipids were extracted from the cells as shown in the legends to Fig. 1 and from NALM-6 cells (*N*), and separated by TLC. The plates were immunostained with antisera from Balb/c mice immunized with the suspension of irradiated ACHN cells, Vero cells, Karpas cells, and EL4 cells

Since EL4 cells are derived from C57BL/6 mice, no immune responses to EL4 cells or EL4 cell components should be usually induced in syngeneic C57BL/6 mice. However, the injection of C57BL/6 mice with the EL4 rafts resulted in production of anti-raft antibodies in syngeneic mice as shown above. We therefore tried using flow cytometry to corroborate that injection of raft suspensions can induce anti-raft antibody production in syngeneic mice. The results showed that the antisera of C57BL/6 mice injected with rafts of syngeneic melanoma cell line B16F1 bound to B16F1 cells (Fig. 5a). Both mouse myeloma cell line P3U1 and lymphoma cell line RL-2 are derived from Balb/c mice, and antisera from Balb/c mice injected with rafts of these syngeneic P3U1 (Fig. 5b) and RL-2 rafts (Fig. 5c) were also confirmed to bind to P3U1 cells and RL-2 cells, respectively. Injection of mice with a PBS suspension of irradiated syngeneic cells did not result in the production of antisera that bound to syngeneic cells (data not shown).

Since repeated immunization of self- or syngeneic antigens is thought to induce autoimmune diseases, we repeated injection of C57BL/6 mice with EL4 rafts or Balb/c mice with the P3U1 rafts and investigated whether the mice produced anti-DNA antibodies by ELISA. The average A_{450} of anti-ssDNA IgM in the sera of the mice injected with PBS and the syngeneic rafts was 0.247 ± 0.027

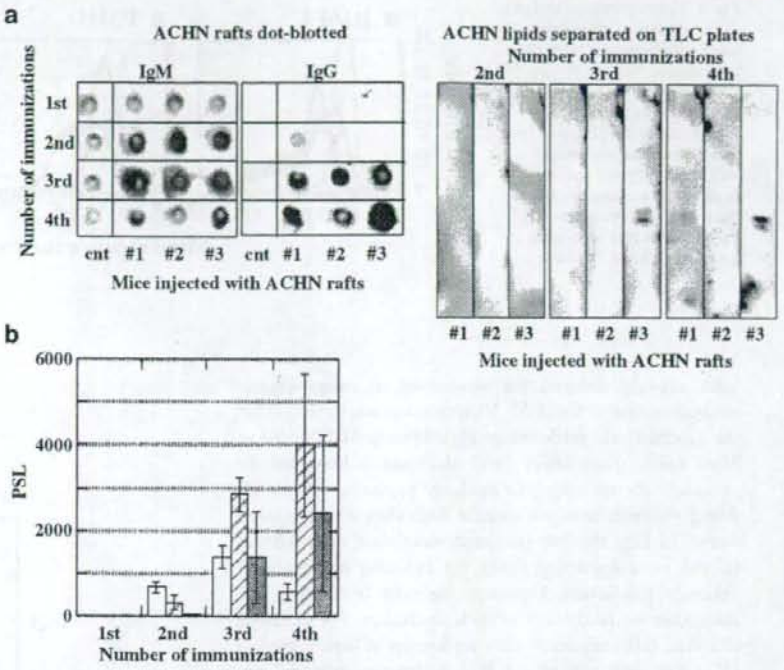

Fig. 3 Kinetics of production of antibody against ACHN rafts. Balb/c mice were injected with an ACHN raft suspension in triplicate (*#1, #2, #3*) or PBS (*cnt*) four times at 7 day intervals, and the sera were obtained 5 days after each immunization. The rafts dot-blotted on PVDF membranes were probed with each antiserum, and then probed with the HRP-conjugated anti-mouse IgM μ chain-specific antibodies or IgG γ chain-specific antibodies as secondary antibody. The lipids separated on the TLC plate were probed with each antiserum, and then with the HRP-conjugated anti-mouse IgG+M antibodies. **a** The images of dot-blot immunostaining of ACHN rafts (*left*) and TLC immunostaining of ACHN lipids (*right*) with the antisera. **b** Measurement of anti-raft IgM antibodies (*open column*), the anti-raft IgG antibodies (*striped column*), and anti-sialylGb5 antibodies (*shaded column*)

(column 1 in Fig. 6) and 0.240±0.043 (column 2 in Fig. 6), respectively, and the difference between the two groups was not significant. The A_{450} for anti-ssDNA IgM in the serum of NZB/WF1, which are well known to spontaneously develop autoimmune disease, was 0.325. No elevation of IgG class anti-DNA antibodies or anti-dsDNA antibodies was observed in the sera of either the immunized mice or NZB/WF1 mice (data not shown). No anti-DNA antibody production or other diagnostic signs of autoimmune disease were observed in these mice. These results show that the development of antibodies against syngeneic rafts components by the mice was not due to the development of an autoimmune disease.

The results of this study show that subcutaneous injection of mice with rafts prepared from specific cell lines induces production of antibodies that recognize single glycolipids, namely monoglycolipid-specific antibodies. For example, rafts prepared from ACHN cells and Vero

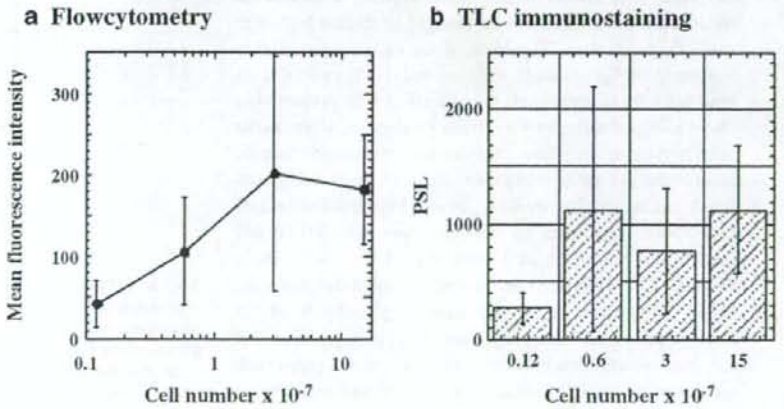

Fig. 4 Reactivity of mouse sera after immunization with the rafts prepared from various numbers of EL4 cells. The sera were obtained from C57BL/6 mice immunized with rafts prepared from 0.12, 0.6, 3 and 15×10^7 EL4 cells. The experiments were performed in triplicate. **a** Evaluation of antibody reactivity to EL4 cells by flowcytometry. **b** Evaluation of antibody reactivity to GD2 by TLC immunostaining

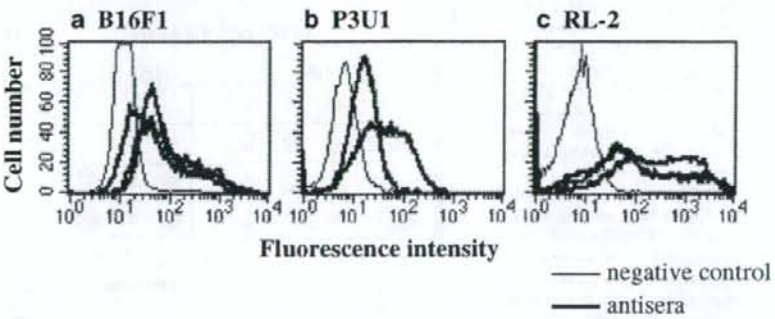

Fig. 5 Flow cytometric analysis of the antisera of mice immunized with syngeneic rafts. Cells were stained with the antisera of C57BL/6 mice immunized with B16F1 rafts (**a**), Balb/c mice immunized with P3U1 rafts (**b**) and Balb/c mice immunized with RL-2 rafts (**c**), and analyzed by flow cytometry (*bold line*). The sera of each mouse injected with PBS were used as a negative control (*thin line*)

cells strongly induced the production of mono-specific antibodies against sialyGb5. However, since sialyGb5 is not the quantitatively predominant glycolipid in ACHN cells or Vero cells, quantitative lipid dominance may not be necessary for monospecific antibody production. Since all four glycolipids to which specific antibodies were produced shown in Fig. 1b were sialylated, sialylation is thought to be the most important factor for inducing monospecific antibody production. However, the rafts from other cell lines gave no production of such antibodies. For example, although B16 melanoma cells are known to highly express GM3 [8], injection of the B16 melanoma rafts did not induce monoglycolipid-specfic antibody. Since Kawashima *et al.* [9] reported that when they intravenously injected ten strains of inbred mice with 100 μg of gangliosides adsorbed to *Salmonella minnesota*, gangliosides such as GD3, GD2, GD1b, GT1a, and GQ1b that have a trisaccharide sequence of NeuAcα2,8NeuAα2,3Gal induced high-titer antibody responses, whereas gangliosides such as GM4, GM3, GM2, GM1, GD1a, and GT1b that have a disaccharide sequence of NeuAcα2,3Gal induced low-titer antibody responses, the diversity of immunogenicity among the glycolipids should be present. Since SSEA-4, an epitope carried by sialyGb5 has been well known highly immunogenic, a saccharide sequence of sailylGb5 can be thought to induce high-titer antibody production. Therefore, if the cells contain highly immunogenic glycolipids such as sialyGb5 and GD2 in lipid rafts, these glycolipids may be effectively presented as immunological targets for antibody production, whereas the rafts containing only low immunogenic glycolipids may be insufficient for antigen presentation to produce anti-glycolipids antibodies. Yamazaki Y. *et al.* [10] obtained several monoclonal antibodies by injecting mice with HL60 cell lipid rafts. One of the antibodies reacted with both GM1a and GD1b, and another reacted with phosphatidylglucoside. HL60 cells, however, mainly express glycolipids of the neolactoseries, not the ganglioseries [11], suggesting that raft immunization enables antibody production against such an extremely minor glycolipid. In order to induce effective

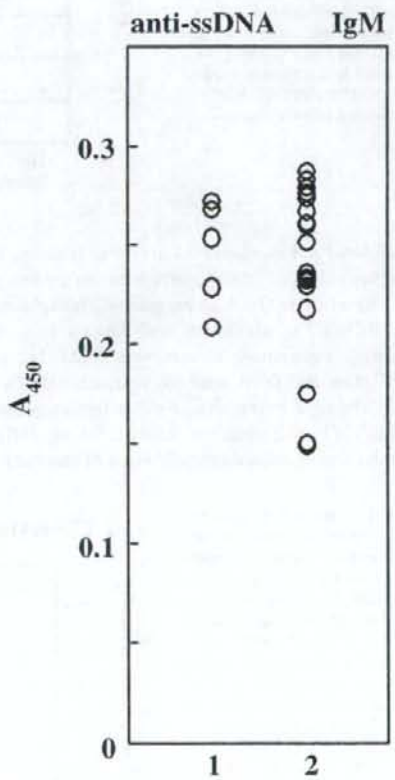

Fig. 6 ELISA of anti-ssDNA antibodies in the sera of mice immunized with syngeneic rafts. Calf thymus ss-DNA was coated and probed with the serum of C57BL/6 or Balb/c mice injected with PBS (*column 1*) and C57BL/6 mice injected with EL4 rafts or Balb/c mice injected with P3U1 rafts (*column 2*). The mean values of triplicate experiments are shown

immune responses against glycolipids in mice, a large amount of purified antigen usually must be immobilized by adsorbing it to the cell walls of bacteria, such as *Salmonella minnesota*, or by incorporating it into liposomes [12], whereas rafts themselves are insoluble and do not need to be immobilized. Furthermore, without mixing with Freund's adjuvant, rafts may retain adjuvant effects and be capable of inducing an immune response even in syngeneic mice.

It still remains unclear how monoglycolipid-specific antibodies are produced, which cells should be used for raft preparation, and to which glycolipids antibodies are predominantly produced. Although further experiments are certainly needed to answer these questions, raft immunization can be used as an effective method of producing monoclonal antibodies against glycolipids and can be applied as new approach in many fields.

Acknowledgments We thank Ms. S. Yamauchi for her excellent secretarial work. This work was supported in part by Health and Labour Sciences Research Grants and Grant for Child Health and Development from the Ministry of Health, Labour and Welfare of Japan, a grant from the Japan Health Sciences Foundation for Research on Health Sciences Focusing on Drug Innovation, JSPS. KAKENHI 18790263, the Budget for Nuclear Research of the Ministry of Education, Culture, Sports, Science and Technology, based on screening and counseling by the Atomic Energy Commission. This work was also supported by CREST, JST, and a grant from Charitable Trust Japan Leukemia Research Fund.

References

1. Katagiri, Y.U., Mori, T., Nakajima, H., Katagiri, C., Taguchi, T., Takeda, T., Kiyokawa, N., Fujimoto, J.: Activation of Src family kinase yes induced by Shiga toxin binding to globotriaosyl ceramide (Gb3/CD77) in low density, detergent-insoluble microdomains. J. Biol. Chem. **274**, 35278–35282 (1999)
2. Katagiri, Y.U., Ohmi, K., Katagiri, C., Sekino, T., Nakajima, H., Ebata, T., Kiyokawa, N., Fujimoto, J.: Prominent immunogenicity of monosialosyl galactosylgloboside, carrying a stage-specific embryonic antigen-4 (SSEA-4) epitope in the ACHN human renal tubular cell line—a simple method for producing monoclonal antibodies against detergent-insoluble microdomains/raft. Glycoconj. J. **18**, 347–353 (2001)
3. Asanuma, H., Takahashi, S., Ishikawa, M., Kamiguchi, K., Sato, N., Poppema, S., Fujimoto, J., Kikuchi, K.: A monoclonal antibody, 3G12, reacts with a novel surface molecule, Hal-1, with high expression in CD30-positive anaplastic large cell lymphomas. Br. J. Haematol. **106**, 55–63 (1999)
4. Katagiri, Y.U., Kiyokawa, N., Nakamura, K., Takenouchi, H., Taguchi, T., Okita, H., Umezawa, A., Fujimoto, J.: Laminin binding protein, 34/67 laminin receptor, carries stage-specific embryonic antigen-4 epitope defined by monoclonal antibody Raft.2. Biochem. Biophys. Res. Commun. **332**, 1004–1011 (2005)
5. Iizuka, J., Katagiri, Y., Tada, N., Murakami, M., Ikeda, T., Sato, M., Hirokawa, K., Okada, S., Hatano, M., Tokuhisa, T., Uede, T.: Introduction of an osteopontin gene confers the increase in B1 cell population and the production of anti-DNA autoantibodies. Lab. Invest. **78**, 1523–1533 (1998)
6. Jacob, F.: Mouse teratocarcinoma and embryonic antigens. Immunol. Rev. **33**, 3–32 (1977)
7. Tang, W.R., Kiyokawa, N., Eguchi, T., Matsui, J., Takenouchi, H., Honma, D., Yasue, H., Enosawa, S., Mimori, K., Itagaki, M., Taguchi, T., Katagiri, Y.U., Okita, H., Amemiya, H., Fujimoto, J.: Development of novel monoclonal antibody 4G8 against swine leukocyte antigen class I alpha chain. Hybridoma Hybridomics. **23**, 187–91 (2004)
8. Sawada, M., Moriya, S., Shinehara, R., Satomi, S., Miyagi, T.: Comparative study of sialidase activity and GM3 content in B16 melanoma variants with different metastatic potential. Acta. Biochim. Pol. **45**, 343–349 (1998)
9. Kawashima, I., Nakamura, O., Tai, T.: Antibody responses to gangliosides-series gangliosides in diffeent strains of inbred mice. Mol. Immunol. **29**, 625–632 (1992)
10. Yamazaki, Y., Nagatsuka, Y., Oshima, E., Suzuki, Y., Hirabayashi, Y., Hashikawa, T.: Comprehensive analysis of monoclonal antibodies against detergent-insoluble membrane/lipid rafts of HL60 cells. J. Immunol. Methods **311**, 106–116 (2006)
11. Stroud, M.R., Handa, K., Salyan, M.E., Ito, K., Levery, S.B., Hakomori, S., Reinhold, B.B., Reinhold, W.N.: Monosialogangliosides of human myelogenous leukemia HL60 cells and normal human leukocytes. 1. Separation of E-selectin binding from nonbinding gangliosides, and absence of sialosyl-Le(x) having tetraosyl to octaosyl core. Biochemistry **35**, 758–769 (1996)
12. Kannagi, R.: Monoclonal anti-glycosphingolipid antibodies. Methods Enzymol. **312**, 160–179 (2000)

ELSEVIER

Experimental Hematology

Experimental Hematology 36 (2008) 37–50

Mutated D4-guanine diphosphate–dissociation inhibitor is found in human leukemic cells and promotes leukemic cell invasion

Yuji Nakata[a,b,d], Kensuke Kondoh[a,b,e], Sachiko Fukushima[a], Akinori Hashiguchi[a], Wenlin Du[a], Mutsumi Hayashi[a,b], Jun-ichiroh Fujimoto[c], Jun-ichi Hata[a,c], and Taketo Yamada[a]

[a]*Department of Pathology and* [b]*Department of Pediatrics, Keio University School of Medicine, Tokyo, Japan;* [c]*National Center for Child Health and Development, Tokyo, Japan;* [d]*Department of Medicine, Division Hematology/Oncology, University of Pennsylvania, Philadelphia, Pa., USA;* [e]*Department of Pediatrics, St. Marianna University School of Medicine, Kanagawa, Japan*

(Received 20 December 2006; revised 23 July 2007; accepted 13 August 2007)

Objective. **Rho GTPase may be involved in human cancer invasion via the augmentation of cell motility and adhesion. We report on two point mutations of the D4-guanine diphosphate (GDP)–dissociation inhibitor (GDI) gene, one of the Rho-GDIs, which were found in a human leukemic cell line, Reh, and the mutated D4-GDI functions as an accelerator of leukemic cell invasion.**

Material and Methods. **We investigated the altered activity of GDP dissociation by mutated (mt) D4-GDI and the functions of this mt and wild-type (wt) D4-GDI in invasion. The mice inoculated with wt or mt D4-GDI vector–transfected Raji cells were observed and examined pathologically. Adhesiveness and cell motility of wt or mt D4-GDI vector–transfected Raji cells were examined. Finally, it was examined whether Rho activation was changed by mutation of D4-GDI under the condition of Rho-GDI knockdown.**

Results. **Two point mutations of the D4-GDI gene were found in Reh cells. The region of mutations is conserved among members of the Rho-GDI family at the amino acid level. D4-GDI with two mutations (V68L and V69A) functioned in a dominant negative manner in the inhibition of GDP dissociation from Rho. Severe combined immune-deficient mice inoculated with Raji cells developed hemiparalysis. The Raji cells were present in bone marrow and peripheral blood, and hepatic invasion was observed in 20% of the mice. Mice inoculated with wt D4-GDI vector–transfected Raji cells (wt D4) showed later paralysis and none developed hepatic invasion. Mice inoculated with mt D4-GDI–transfected Raji cells (mt D4) showed a 5-day reduction in the time to paraplegia and death. In addition, hepatic invasion was evident in 80% of mice transplanted with mt D4 cells. There were no differences in growth rates and amounts of guanine triphosphate (GTP)–bound Rho, cdc42, or Rac among all clones, however, GTP-bound Rho in mt D4 clone with short hairpin RNA (shRNA) vector for Rho-GDI knockdown was increased compared with wt D4 clone with shRNA vector for Rho-GDI knockdown. The mt D4 cells showed an augmentation of adhesiveness and cell motility. On the other hand, wt D4 cells showed a decreased ability of cell motility.**

Conclusion. **These results suggest the mutated D4-GDI functions as a dominant negative molecule against the wt D4-GDI and accelerates invasion via regulation of cytoskeletal machinery.**

Human leukemia progression is a process by which leukemic cells acquire more malignant properties, such as invasiveness. We previously established in vivo experimental systems of human leukemia invasion using severe combined immune-deficient (SCID) mice and reported that Rho activation augmented human leukemic cells invasion and changed the pattern of organs targeted by leukemic cells through the acceleration of leukemic cell adhesion [1].

The Rho, Rac, and Cdc 42 GTPases belong to the small guanine triphosphate (GTP)–binding protein family, a part of the Ras superfamily, and regulate various actin filament–dependent cell functions, such as cell adhesion, cell

Dr. Fukushima's current address: Department of Dermatology, Kanazawa University School of Medicine, Kanazawa, Japan.

Offprint requests to: Taketo Yamada, M.D., Department of Pathology, Keio University School of Medicine, 35 Shinano-machi, Shinjuku-ku, Tokyo 160-8582, Japan; E-mail: taketo@sc.itc.keio.ac.jp

0301-472X/08 $–see front matter.
doi: 10.1016/j.exphem.2007.08.023

motility, and cytokinesis [2–5], as well as certain gene expressions [6]. These GTPases are active only in GTP-bound states and the exchange of GTP and guanine diphosphate (GDP) is strictly regulated by three types of regulatory proteins; GDP dissociation stimulators (GDS), GDP dissociation inhibitors (GDI), and GTPase activating proteins (GAP). Some GDS and GAP from the Rho family and three Rho GDIs have been isolated [7]. D4-GDI, one of the Rho GDIs, is preferentially expressed in hematopoietic cells, and Rho-GDIγ is expressed in the brain, lungs, kidneys, testes, and pancreas, while Rho-GDI is ubiquitously expressed in all mammalian organs [8–10]. Rho-GDI binds the majority of Rho-family GTPases in the cytoplasm, maintaining Rho in an inactive form in which it cannot interact with effecter targets or other regulatory proteins [11]. On the other hand, Rho-GDI also associated weakly with the GTP-bound forms of Rho, Rac, and Cdc42 [12,13]. This weak interaction resulted in an inhibition of the intrinsic and GAP-stimulated GTPase activities of the Rho GTPases. Thus, Rho-GDI appears to be a molecule capable of blocking the GTP binding/GTPase cycle at two points: at the GDP–GTP exchange step and the GTP hydrolytic step. Further studies demonstrated that Rho-GDI associates with a Rho-GDI displacement factor from the ERM family, which consists of ezrin, radixin, and moesin. ERM interacts with both an adhesion molecule—CD44—and F-actin, resulting in association of the actin cytoskeleton with the plasma membrane [14]. D4-GDI has been identified as a Rho-GDI–like protein that is approximately 68% homologous with Rho-GDI, and is preferentially expressed at very high levels in hematopoietic cells, including erythroid, granulocytic, monocytic, and lymphoid cells [8]. In another report, expression of D4-GDI in lymphocytes was emphasized and D4-GDI was named Ly-GDI [9]. The inhibitory effect of D4-GDI on GDP dissociation was specific for Rho, but not Ras or Rap [8]. Like other Rho-GDIs, D4-GDI was postulated to bind and inhibit Rho GTPases. However, much yet remains to characterize the specificity of D4-GDI [15,16].

D4-GDI has been reported to be a substrate of the apoptosis protease CPP32. D4-GDI was rapidly truncated to a 23-kDa fragment in Jurkat cells with kinetics that parallel the onset of apoptosis following Fas cross-linking with agonistic antibody or treatment with staurosporine [17]. Furthermore, Krieser et al. [18] showed that a cleaved 26-kDa fragment derived from D4-GDI resided in the cytoplasm of undamaged cells, whereas after cleavage by CPP32, the 22-kDa form of D4-GDI translocated to the nucleus [18]. These lines of evidence suggest that D4-GDI is involved in cell-shape alterations and/or changes in cell fragmentation during leukocyte apoptosis.

A number of Ras gene mutations have been found in a wide variety of human malignant tumors, including leukemias and lymphomas [19]. Point mutations in Ras cause decreased GTPase activity and may transform in some leukemic cells. Rho, a member of the Ras family, has not been associated with transformation, and no Rho mutations have been detected in human malignant tumors to date [20]. However, it has been reported that some regulatory proteins for Rho GTPases, dbl, tiam1, and vav, are reportedly associated with tumor development [7,21,22]. The Dbl oncogene was originally discovered because of its ability to induce focus formation and tumorigenicity when expressed in NIH-3T3 cells [23]. Tiam, however, was first identified as an invasion-inducing gene using proviral tagging in combination with in vitro selection for invasiveness [24]. Furthermore, the Rho family of small GTPases, including Rac, Cdc42, and Rho, has been implicated in the regulation of many aspects of cancer cell motility and invasion, including cell polarity, cytoskeletal organization, and transduction of signals from the extracellular environment [25–28].

In this study, we identified two point mutations of the D4-GDI gene in a human B-cell leukemia cell line, Reh, and analyzed the functions of the mutated (mt) D4-GDI in vitro and in vivo employing an experimental system consisting of human leukemic cell invasion in SCID mice.

Materials and methods

Human leukemic cells and cell culture

Two acute lymphoblastic leukemia cell lines (Reh and HPB-ALL) and three Burkitt's lymphoma cell lines (Raji [ATCC, CCL-86], Ramos [ATCC, CRL-1923], and Daudi [ATCC, CCL-213]) were examined. The Reh cell line was established from a girl with a common form of acute lymphoblastic leukemia [29]. This cell line is known to be accompanied by the TEL-AML1 fusion gene due to chromosomal translocation [30]. We used reverse transcriptase polymerase chain reaction (RT-PCR) to confirm that our Reh cells expressed mRNA derived from the TEL-AML1 fusion gene (data not shown). The Raji cell line was derived from Burkitt's lymphoma. The HPB-ALL cell line was derived from a pediatric T-cell leukemia [31]. Cells were cultured in the presence of 5% CO_2 at 37°C using RPMI-1640 medium supplemented with 10% fetal bovine serum. Normal human peripheral blood lymphocytes from healthy Japanese men were also examined with informed consent.

RT-PCR and DNA sequencing

Total RNA was extracted from each sample (5–10 × 10^6 cells) using ISOGEN (Nippon Gene, Toyama, Japan). RNA was reverse-transcribed into first strand cDNA using a First-Strand cDNA Synthesis Kit (Amersham-Pharmacia Biotech, Buckinghamshire, UK). D4-GDI cDNA was isolated by PCR amplification from first-strand cDNA using the N-terminal primer (5′-TAAATA GATCAGAATGACTGAA-3′) and the C-terminal primer (5′-AGAATTCTTCCA AGGTGGCAA-3′). PCR was performed in 10 mM Tris-HCl (pH 9.0), 2.0 mM $MgCl_2$, 50 mM KCl, 0.2 mM each deoxyribonucleoside triphosphate, and 0.5 μM each PCR primer using Taq DNA Polymerase (Toyobo, Tokyo, Japan). Thirty cycles were run with denaturation at 94°C for 60 seconds, annealing at 55°C for 60 seconds, and extension at 72°C for 60

seconds. RT-PCR products were cloned into a pGEM-T vector (Promega, Madison, WI, USA), and analyzed with a Thermo Sequenase fluorescent-labeled primer cycle sequencing kit (Amersham-Pharmacia Biotech) using T7 and Sp6 fluorescent primer and a DNA sequencer (MegaBase 1000, Molecular Dynamics, Sunnyvale, CA, USA). The fluorescent primers used for sequencing were forward, 5′-GTCGCAGGAA ATGGACA AAGAT-3′ and reverse 5′-TCCAGTAA GGTCCATG GTGATT-3′.

Sequences of genomic D4-GDI DNA

DNA was prepared from Reh cells by standard methods with sodium dodecyl sulfate–proteinase K [32]. A portion of the D4-GDI gene that included the mutations was amplified using the N-terminal primer (5′-CACCACAGAAGTCCCTGAAAGA-3′) and the C-terminal primer (5′-TCCA GTAAGGTCCATGGT GATT-3′). PCR products were cloned into a pGEM-T vector and sequenced. After partial sequencing of the D4-GDI intron (data not shown), PCR products were analyzed by direct sequencing methods using the fluorescent forward primer (5′-CACCCAC TATACACATGTCTCT-3′) for the D4-GDI gene intron. Reh cells were also obtained from other laboratories and the D4-GDI gene was sequenced by the following method in order to eliminate any contamination of cells and to confirm the mutations. RT-PCR was performed with another N-terminal primer (5′-ACAGA GACGTGAAGCACTGAA-3′) and C-terminal primer (5′-GATG CATCAA TAAGGAAATGT-3′). These primers flanked the initial primers and were used to exclude contamination of PCR products and plasmids. PCR products were analyzed by direct sequencing method.

Construction of mt and wild-type D4-GDI expression vectors and short hairpin RNA vector for knockdown of Rho-GDI-α

Mutated D4-GDI cDNA of Reh cells was generated by RT-PCR. Wild-type (wt) D4-GDI cDNA was generated from HPB-ALL cells by RT-PCR. Vectors containing wt or mt D4-GDI cDNA with a myc-tag driven by the SRα promoter were constructed. This vector contained the neomycin-resistance (neo^r) gene driven by the SV40 promoter. The specific sequences for Rho-GDI small interfering RNA were searched by siDirect online software (RNAi Corporation, Tokyo, Japan). As a result, nucleotide number of human Rho-GDI-α 1191–1213 (3′UTR TCGGTCCCGTCTAAC CATGATGC) as Rho-GDI-α and scramble 23-nucleotide as control were generated. DNA-based small interfering RNA vectors were constructed in pBLOCK-iT6 DEST vector (Invitrogen, Carlsbad, CA, USA) for short hairpin RNA (shRNA) synthesis.

Transfection of wt or mt D4-GDI gene and shRNA vector for Rho-GDI knockdown into Raji cells

Wild-type or mt D4-GDI expression vector or shRNA vector for Rho-GDI knockdown was transfected into Raji cells by electroporation using a Gene Pulser (Bio-Rad, Hercules, CA, USA). The SRα-myc-tag vector or shRNA vector with scramble 23-nucleotide was transfected into Raji cells as a control. The Raji cells were cultured in culture media with G418 (800 μg/mL; Sigma-Aldrich, Tokyo, Japan) or blasticidin (10 μg/mL; Invitrogen, Carlsbad, CA, USA) for 14 days, followed by subcloning in a 96-well plate twice. Expression of D4-GDI or Rho-GDI-α protein was confirmed by Western blotting using a rabbit anti-D4-GDI or Rho-GDI polyclonal antibody (Zymed Laboratory, San Francisco, CA, USA). Blotted membranes were treated with peroxidase-conjugated anti-rabbit immunoglobulin antibody and visualized with electrochemiluminescence (Amersham-Pharmacia Biotech). The protein concentration was measured by BCA protein assay reagent (Pierce, Rockford, IL, USA).

Transplantation of leukemic cells into SCID mice

SCID mice (C.B.17 SCID mice, female, 7 to 9 weeks after birth; Clea, Tokyo, Japan) were maintained under specific pathogen-free conditions, and 2×10^7 Raji cells with/without wt or mt D4-GDI or Rho-GDI shRNA were suspended in 100 μL culture medium and injected into the tail veins of mice.

Analysis of leukemic cell invasion in SCID mice

Development of hemiparalysis in the mice was defined as the state in which they showed no motion of their hemilateral lower extremities. On day 17 or 20, when all mice were still alive and some showed hemiparalysis, the mice were sacrificed. Peripheral blood was prepared from the orbital vein plexus and cells were taken from the bilateral femurs and tibiae, and the spleen. The peripheral blood was subjected to hemolysis before being washed in phosphate-buffered saline (pH 7.4). Samples were then subjected to staining with anti-human CD19 monoclonal antibody (phycoerythrin-conjugated; DAKO, Glostrup, Denmark, diluted 1:100) for analysis with a flow cytometer (EPICS XL-MCL; Beckman Coulter, Hialeah, FL, USA). The systemic organs of mice were also prepared for pathological analysis by fixation in 10% formaldehyde in phosphate-buffered saline, embedding in paraffin, sectioned and then stained with hematoxylin-eosin. Immunohistochemical analyses were performed with anti-human CD19 monoclonal antibody and anti-proliferating cell nuclear antigen (PCNA) monoclonal antibody (Oncogene Science, Uniondale, NY, USA, diluted 1:50).

In vitro and in vivo proliferation assay

Proliferation rates of Raji cells with mt or wt D4-GDI or myc-tag only and shRNA vector for Rho-GDI knockdown or scramble 23-nucleotide were determined using the MTT method. These three clones were placed in eight wells of a round-bottomed 96-well plate at a concentration of 2×10^3 cells/100 μA/well and cultured for 48 hours, followed by addition of 5 mg/mL MTT (3-[4,5-dimethylthiazol-2-yl]-2,5-diphenyltetrazolium bromide; Sigma-Aldrich) at a concentration of 10 μL/well and further cultured for 4 hours. After the cells had settled on the plate, 100 μL 0.04 N HCl plus isopropanol was added. The resultant mixture was stirred and then measured using an enzyme-linked immunosorbent assay reader (Microplate Reader Model 450; Bio-Rad) for absorbance at 570 nm and 630 nm.

The in vivo proliferative capabilities of leukemic cells were investigated by the PCNA labeling index in situ [33]. The number of nuclear PCNA-positive cells and total cells in the vertebrae were counted in 10 fields.

Cell motility assay

Cell migration ability was assessed in 48-well chambers using polyvinylpyrrolidone-free polycarbonate membranes with 5-μm or 3-μm pores (NeuroProbe, Inc., Gaithersburg, MD, USA). RPMI-1640 supplemented with 1% pasteurized human plasma was placed in lower wells, and used to dilute the cells in upper wells. After 3 hours at 37°C, the membrane was removed, washed on the upper side with phosphate-buffered saline, then fixed and stained with DiffQuik (NeuroProbe). All assays were done in triplicate, and migrated cells were counted in five randomly selected

fields at 600-fold magnification. General and spontaneous migration was determined in the absence of chemokines.

Adhesion assays

Adhesion of Raji cells to the extracellular matrix or cells was assessed. Extracellular matrices (Matrigel; Becton-Dickinson, Mountain View, CA, USA), human fibronectin, laminin, and collagen type IV (Asahi Techno Glass, Funabashi, Chiba, Japan) were used in the 24-well Biocoat cellware (Becton-Dickinson). Human bone marrow stromal cells, which were obtained from bone marrow specimens of nonhematological patients, with informed consent, were seeded in 24-well plates prior to 24-hour adhesion assays. Cells were fluorescently labeled with 2 μM 2,7-bis-(2-carboxyethyl)-5 (and 6) carboxyfluorescein (BCECF; Molecular Probes, Eugene, OR, USA) for 30 minutes at 37°C. Labeled cells were washed twice, resuspended with RPMI to achieve a concentration of 2×10^5 cells/mL, and added to each well. After incubation with fixative, plates were washed and the number of fluorescent cells bound was determined by proportionality to the remaining BCECF fluorescence measured using a FluorImager 595 (Molecular Dynamics).

Affinity-precipitation of cellular GTP-bound Rho, Cdc42, and Rac

Ren et al. [34] developed a method based on evidence that Rho effectors interact only with GTP-bound Rho for the measurement of Rho activity [34]. Binding of Rho to the Rho-binding domain (RBD) from the effector protein Rhotekin inhibited both the intrinsic and GAP-enhanced GTPase activity of Rho [35]. Therefore, Rhotekin RBD was used to affinity-precipitate cellular GTP-Rho. Cells were washed with ice-cold Tris-buffered saline and lysed in RIPA buffer (50 mM Tris [pH 7.2], 1% Triton X-100, 0.5% sodium deoxycholate, 0.1% sodium dodecyl sulfate, 500 mM NaCl, 10 mM $MgCl_2$, 10 mg/mL each of leupeptin and aprotinin, and 1 mM phenylmethylsulfonyl fluoride). Cell lysates were clarified by centrifugation at 13,000*g* at 4°C for 10 minutes, and equal volumes of lysates were incubated with GST-RBD (a fusion of RBD with glutathione S-transferase, 20 μg) beads at 4°C for 45 minutes. Beads were washed four times with buffer B (Tris buffer containing 1% Triton X-100, 150 mM NaCl, 10 mM $MgCl_2$, 10 mg/mL each of leupeptin and aprotinin, and 0.1 mM phenylmethylsulfonyl fluoride). Bound Rho proteins were detected by Western blotting using an anti-RhoA monoclonal antibody (Santa Cruz Biotechnology, Santa Cruz, CA, USA). Densitometric analysis was performed using NIH image version 1.62. The amount of RBD-bound Rho was normalized to the total amount of Rho in cell lysates for the comparison of Rho activity (level of GTP-bound Rho) in different samples. Depending on cell conditions and types, and different batches of GST-RBD, the RBD-bound Rho accounts for ~0.5% to 5% of total Rho. The measurement of Rac activity was performed using the Rac Activation Assay kit (Cytoskeleton, Denver, CO, USA) according to the manufacturer's protocol.

[^{3}H]GDP dissociation assay

D4-GDI (wt, V68L, V69A, and both V68L and V69A mutations) protein was synthesized using Baculo-viral expression system with Bac-to-Bac HT vector (Invitrogen, Carlsbad, CA, USA) and Sf9 cells. His-tag D4-GDI proteins in cell lysates were purified using Ni-NTA agarose and ProBond Purification system (Invitrogen) according to the manufacturer's protocol. The inhibitory activities of wt, mt (V68L, V69A, and both V68L and V69A mutations), and wt plus each mt D4-GDI on GDP dissociation from isoprenylated Rho were determined using a filtration assay, as described previously by Chuang et al. [13]

Statistical analysis

All results were evaluated using Student's *t*-test–based statistics. Experiments were performed at least three times each.

Results

Detection of mutations of D4-GDI cDNA or genomic DNA in human leukemic cells

Results of DNA sequence analysis of the D4-GDI cDNA from the human leukemic cell lines are shown in Figure 1. Two point mutations at positions 276 (a G to C change) and 280 (T to C) were found in the D4-GDI cDNA of the Reh cell line. No mutations of the D4-GDI gene were detected in the D4-GDI genes of HPB-ALL, Raji, Ramos, and Daudi cell lines or in normal human peripheral blood lymphocytes (data not shown). Direct sequencing analysis of genomic DNA showed that these mutations were present on one allele (Fig. 2). These two point mutations of D4-GDI in the Reh cell led to conversions of valine 68 to leucine and valine 69 to alanine. The alignment of the predicted amino acid sequences of mt D4-GDI, wt D4-GDI, and other Rho-GDI family genes are shown in Figure 1. These two mutations exist in the partially conserved region at the amino acid level.

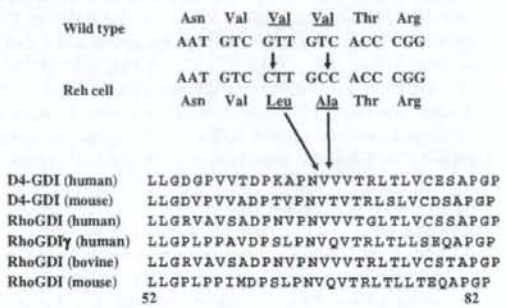

Figure 1. Two point mutations of D4-GDI cDNA in Reh cells and alignment of the predicted amino acid sequence. Two point mutations in D4-GDI were detected in Reh cells (arrows). These changes resulted in a guanine to cytosine substitution at position 276 and a thymine to cytosine substitution at nucleotide 280 (underlined). The alignment of predicted amino acid sequences of D4-GDI and Rho-GDI family genes. The two D4-GDI point mutations in Reh cells led to a valine 68 to leucine change and a valine 69 to alanine change. This region is highly conserved in Rho-GDI family members.

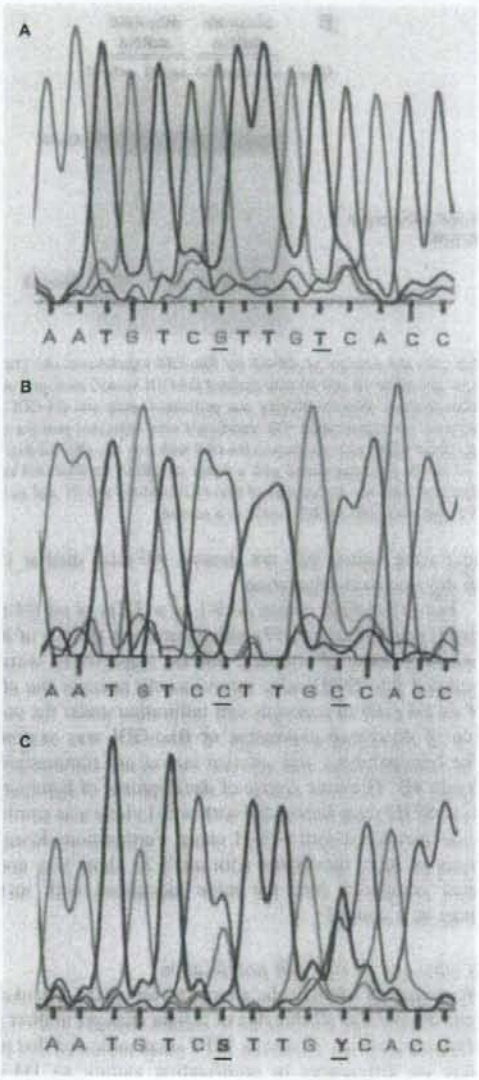

Figure 2. Heterozygous mutations of the D4-GDI gene in Reh cells. (**A**) Normal D4-GDI sequence from normal human peripheral blood lymphocytes. (**B**) Two point mutations in D4-GDI in Reh cells (underlined). These changes resulted in a guanine to cytosine substitution at position 276 and a thymine to cytosine substitution at nucleotide 280. (**C**) Direct sequence analysis of DNA amplified from genomic DNA of Reh cells showed identical mutations in one allele (heterozygous). Arrowheads indicate the two peaks, guanine and cytosine at position 276, and thymine and cytosine at nucleotide 280.

Gene transfer of wt or mt D4-GDI expression vector into Raji cells

A human leukemic cell line (Raji) was used in order to clarify the functions of mt or wt D4-GDI, because there were no mutations of D4-GDI gene in the Raji cells. Some clones with wt D4-GDI, mt D4-GDI, or the myc-tag vector were obtained and used in subsequent experiments. Expression of exogenous D4-GDI in these clones was confirmed by Western blotting using anti–D4-GDI polyclonal antibody. These cells expressed a protein of approximately 29 kDa, which was recognized by the D4-GDI antibody (Fig. 3A). The lower bands were endogenous D4-GDI in Raji cells and the upper bands were the exogenous D4-GDI with the myc-tag. We detected the expression of exogenous D4-GDI protein by Western blotting using anti-myc-tag antibody (9E10) (data not shown). The amounts of exogenous D4-GDI were almost the same as the endogenous D4-GDI in clones 21 and 26 with wt D4-GDI and in clone 13 with mt D4-GDI.

Gene transfer of a shRNA vector for Rho-GDI knockdown into Raji cell clones with wt or mt D4-GDI expression vector

The Raji cells with the wt D4-GDI (clone 3) or the mt D4-GDI (clone 13) were transferred with a shRNA vector for Rho-GDI knockdown or a vector of scramble shRNA as a control. Clones that were selected by blasticidin were examined by Western blotting using anti–Rho-GDI polyclonal antibody. Expression of Rho-GDI in clone wt3-21 and mt13-27 with Rho-GDI shRNA vector was decreased compared with clone wt3-1 and mt13-3 with scramble shRNA vector as a control (Fig. 3B). The clones with decreased expression under a quarter of Rho-GDI were established from the Raji cells with the wt D4-GDI, on the other hand, clones with a decreased expression under a half of Rho-GDI were not obtained from the Raji cells with the mt D4-GDI.

Exogenous D4-GDI expressions alter invasion of human leukemic cells in SCID mice

Wild-type D4-GDI clones (21 and 26), mt D4-GDI clones (13 and 20), and two myc-tag clones (1 and 4) were inoculated into SCID mice intravenously. The hemiparalysis and survival curves are summarized in Figure 4A. All mice (n = 18) inoculated with the myc-tag clone (as a control) developed hemiparalysis at 18 to 41 days (mean: 24 days) after transplantation. Histological analysis of systemic organs on day 20 revealed that the myc-tag clones invaded the liver in two of the nine mice (22%). Myc-tag clones were present in peripheral blood (3–52% of white blood cells) and bone marrow (3–66% of mononuclear cells) on day 20. Myc-tag clones infiltrated both ovaries, as well. There were no invasions of myc-tag clones into the brain, salivary glands, lungs, kidneys, digestive tract, heart, adrenal glands, spleen, or thymus. In the mice with hemiparalysis, numerous monotonous blasts occupied the bone marrow of vertebrae and femora, and also extended beyond the bone into the epidural space of the spinal cord, and into neighboring muscles (Fig. 5A). The murine hematopoiesis in bone marrow was markedly suppressed

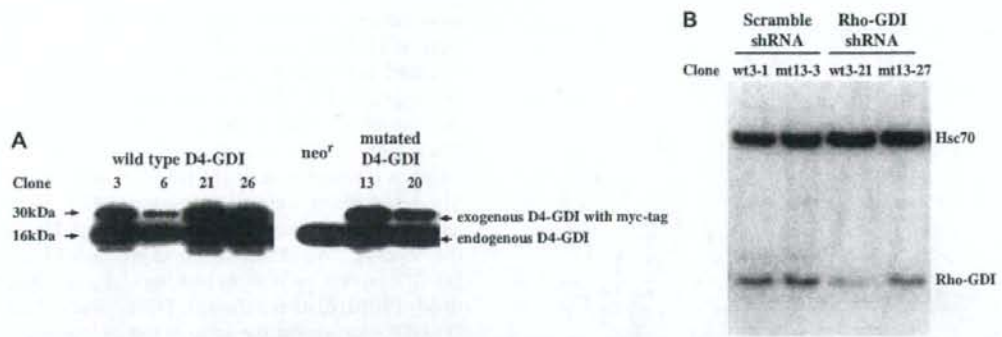

Figure 3. Gene transfer of wild-type or mutated D4-GDI expression vector into Raji cells and a vector of shRNA for Rho-GDI knockdown. (**A**) The Raji cells carrying the D4-GDI gene (clones 3, 6, 21, and 26 with wild-type D4-GDI vector and clone 13 and 20 with mutated D4-GDI vector) were prepared in Laemmeli's buffer and resolved by sodium dodecyl sulfate polyacrylamide gel electrophoresis. Western blotting was performed using anti-D4-GDI polyclonal antibody, peroxidase-conjugated secondary antibody, and electrochemiluminescence for visualization. The transfected cells expressed proteins of approximately 29 kDa and 30 kDa. The 29-kDa bands were endogenous D4-GDI and the upper bands were exogenous D4-GDI with myc tag. (**B**) The Raji cells with the wild-type (wt) D4-GDI (clone 3, wt3) or the mutated (mt) D4-GDI (clone 13, mt13) were transferred with a vector of shRNA for Rho-GDI knockdown. Selected clones were examined by Western blotting using anti-Rho-GDI polyclonal antibody. Expression of Rho-GDI in clone wt3-21 and mt13-27 with Rho-GDI shRNA vector was decreased compared with clone wt3-1 and mt13-3 with scramble shRNA vector as a control.

by infiltration of human leukemic cells. In addition, the spinal cord showed spongiosis, suggesting that development of hemiparalysis in these mice was attributable to invasion of the epidural space by leukemic cells (Fig. 5A). All mice inoculated with myc-tag clones died at 20 to 43 days posttransplantation.

Hemiparalysis in SCID mice inoculated with wt D4-GDI clones was apparently delayed as compared with the mice inoculated with myc-tag clones. These mice developed hemiparalysis (Fig. 4A). Eighteen of the 26 had hemiparalysis at 18 to 49 days (mean: 33.9 days, $p < 0.01$) after transplantation. Some of the SCID mice inoculated with wt D4-GDI clones developed hemiparalysis during the 60-day observation period (69% of all mice). The remaining mice survived more than 60 days (31% of all mice). There were no invasions of Raji cells with wt D4-GDI overexpression in the liver on day 20 after transplantation (0 of the 6 mice). The wt D4-GDI clones were present in peripheral blood (3–9% of white blood cells) and bone marrow (4–10% of white blood cells) on day 20.

On the other hand, SCID mice inoculated with mt D4-GDI clones began to develop hemiparalysis earlier, i.e., on day 14, after transplantation as compared with the mice inoculated with myc-tag clones, which developed similar paralysis after day 18 posttransplantation (Fig. 4A). All mice with mt D4-GDI (n = 20) developed hemiparalysis at 14 to 20 days (mean: 17.4 days, $p < 0.01$) after transplantation.

Histological analysis of mice inoculated with the mt D4-GDI clones revealed hepatic invasion of leukemic cells on day 17 in 8 of the 10 mice (80%), and all had larger invasive areas than the control myc-tag mice (Fig. 5B and C). Furthermore, invasions of Raji cells into the brain, kidneys, and ovaries in some of the mt D4-GDI clone–transplanted mice were found (date not shown). All mice died at 17 to 26 days posttransplantation.

The wt D4-GDI clones (wt3-1 or wt3-21) or mt D4-GDI clones (mt13-3 or mt3-27) with a vector for shRNA of Rho-GDI or a vector of scramble shRNA, respectively, were inoculated into SCID mice intravenously because the effect of mt D4-GDI in leukemic cell infiltration under the condition of decreased expression of Rho-GDI was examined. The hemiparalysis and survival curves are summarized in Figure 4B. The time course of development of hemiparalysis in SCID mice inoculated with wt3-1 clone was similar to mice inoculated with wt3-21 clone. Furthermore, hemiparalysis of mice inoculated with mt13-27 clone was not altered compared with the mice inoculated with mt13-3 clone as a control.

In vitro and in vivo cell proliferation

We examined whether the altered invasiveness of leukemic cells in vivo was attributable to certain changes in their proliferative abilities. However, MTT assay indicated that there were no differences in proliferation among wt D4-GDI clones, mt D4-GDI clones, and myc-tag clones in vitro (Fig. 6). An immunohistochemical analysis using anti-PCNA antibody was done in order to identify the proportion of in situ leukemic cells in S phase. PCNA is expressed in the nuclei of cells in the S phase in parallel with incorporation of bromodeoxyuridine or [^{3}H]-thymidine [1,33]. Almost all PCNA-positive cells in the bone marrow were human leukemic cells. There were no significant differences among the PCNA-labeling indices of wt D4-GDI clones, mt D4-GDI clones, and myc-tag clones (data not shown). These results indicate that neither wt nor mt D4-GDI expression altered leukemic cell invasion via induction of cell proliferation. The proliferating activity of the wt

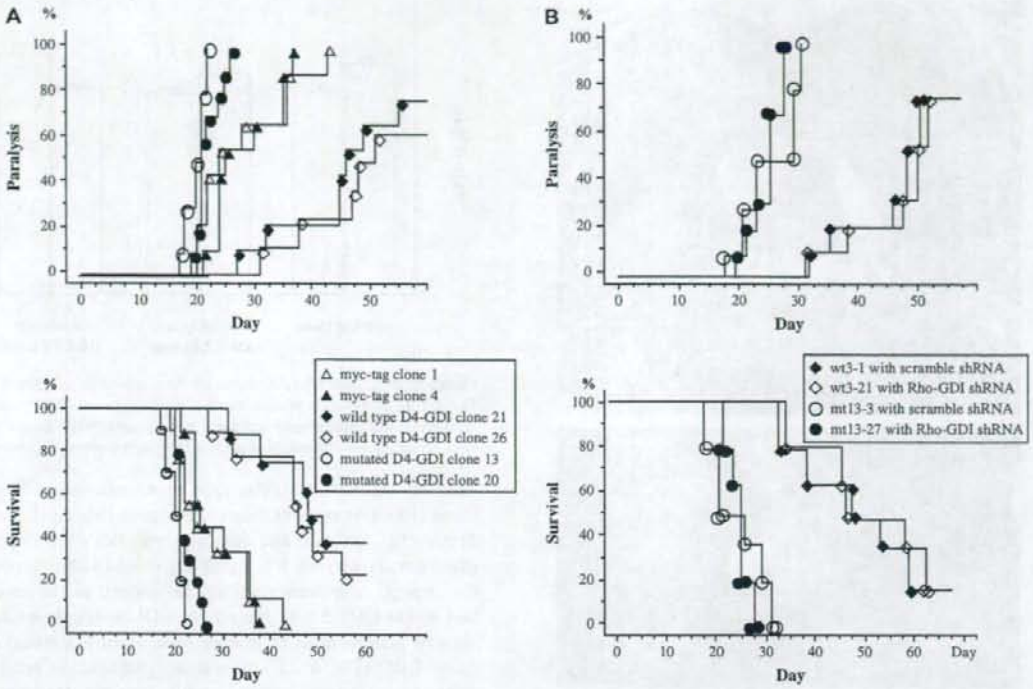

Figure 4. Alteration of hemiparalysis and survival with exogenous D4-GDI expressions in leukemic cells. (**A**) Hemiparalysis was observed in severe combined immune deficient (SCID) mice inoculated with wild-type D4-GDI clones (21 and 26), mutated D4-GDI clones (13 and 20) and myc-tag clones (1 and 4). The mice inoculated with wild-type D4-GDI clones developed hemiparalysis later than myc-tag clone–transplanted mice. On the other hand, the mutated D4-GDI clone–transplanted mice developed hemiparalysis earlier than the myc-tag clone–transplanted mice. Data on the appearance of hemiparalysis; Myc-tag clone transplanted mice (n = 18) at 18 to 41 days (mean: 24 days), wild-type D4-GDI–transplanted mice (n = 26) at 18 to 49 days (mean: 33.9 days, $p < 0.01$), and mutated D4-GDI–transplanted mice (n = 20) at 14 to 20 days (mean: 17.4 days, $p < 0.01$) after transplantation. (**B**) The wild-type D4-GDI clones (wt3-1 or wt3-21) or mutated D4-GDI clones (mt13-3 or mt3-27) with a vector for shRNA of Rho-GDI or a vector of scramble shRNA were inoculated into SCID mice. The hemiparalysis and survival curves are not altered. The time course of development of hemiparalysis in SCID mice inoculated with wt3-1 clone was similar to mice inoculated with wt3-21 clone. The hemiparalysis of mice inoculated with mt13-27 clone was not altered compared with the mice inoculated with mt13-3 clone as a control.

D4-GDI clones (wt3-1 or wt3-21) or mt D4-GDI clones (mt13-3 or mt3-27) with a vector for shRNA of Rho-GDI or a vector of scramble shRNA were examined using MTT assay in order to observe the function of mt D4-GDI under the condition of decreased expression of Rho-GDI. As a result, no differences between these clones (wt3-1, wt3-21, mt13-3 or mt3-27) were revealed (data not shown).

Alteration of cellular motile activity by exogenous D4-GDI expression

We attempted to estimate changes in general cell motility in response to exogenous D4-GDI expression in leukemic cells, because we did not detect differences in cell proliferation of wt or mt D4-GDI clones in vitro or in vivo. As a result, mt D4-GDI clones had increased cell motilities ($p < 0.001$), and wt D4-GDI clones had decreased cell motilities ($p < 0.01$) as compared with the myc-tag clones, without chemokines in vitro (Fig. 7). The cellular motile activities of each clone would correspond to the invasive activities (see Figs. 4 and 5). Mutated D4-GDI clone 13 showed the highest motile activity in vitro and the highest invasive activity in vivo. The motile activity of wt or mt D4-GDI clones (wt3-1, wt3-21, mt13-3, or mt3-27) with a vector of scramble shRNA or a vector for shRNA of Rho-GDI were examined in order to analyze the function of mt D4-GDI under the condition of decreased expression of Rho-GDI. As a result, no alterations between clone wt3-1 and wt3-21, or between clone mt13-3 and mt3-27, were observed (data not shown).

Augmentation of cell adhesion by mt D4-GDI expression

Cell motility consists of multiple and complex steps, including a response against chemotactic factors, cytoskeletal organization, and cell adhesion. We investigated whether exogenous D4-GDI expression altered the motile activity of leukemic cells through changes in cell adhesion. Adhesion of Raji cells, which contain mt or wt D4-GDI or the

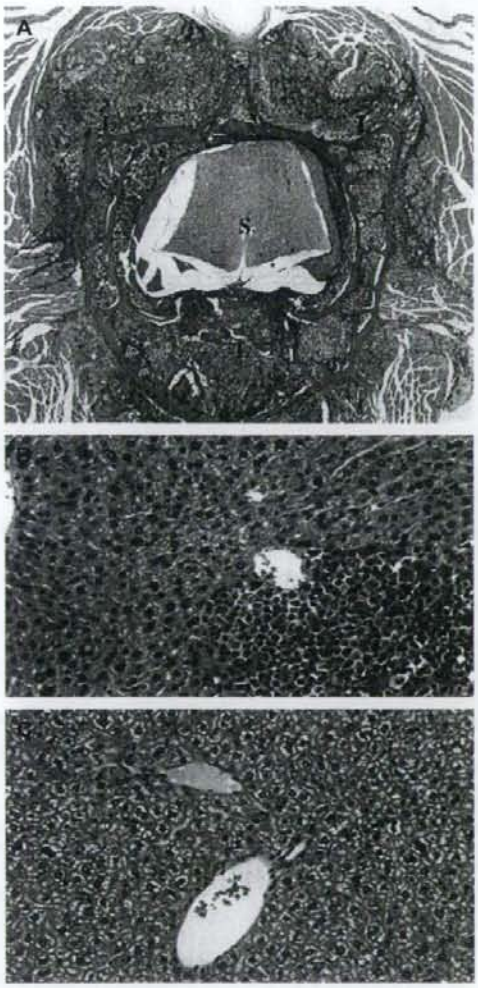

Figure 5. Raji cell invasion in severe combined immune deficient (SCID) mice. (**A**) The vertebra of an SCID mouse inoculated with myc-tag clone 1 is shown in a transverse section (hematoxylin-eosin staining). Raji cells have invaded the bone marrow, surrounding tissues, and the epidural space (day 17 after transplantation). The result is spongiosis, due to compression myelopathy of the spinal cord. S and L indicate the spinal cord and human leukemic (Raji) cells, respectively. Original magnification ×100. (**B**) Hepatic invasion by mutated D4-GDI clone 13 is shown. Original magnification ×120. (**C**) On other hand, there was no hepatic invasion in mice inoculated with wild-type D4-GDI clone 26. Original magnification ×120.

myc-tag only, to the extracellular matrix or cells was assessed as described previously [1]. Extracellular matrices (Matrigel [Becton-Dickinson], human fibronectin, laminin, and collagen type IV) were placed in 24-well dishes. In order to quantitate cell-adhesion activity, the leukemic cells were labeled with 2 μM BCECF, washed, and the fluorescence was then measured with a FluorImager 595. As a result, no significant differences in adhesiveness between these clones on each extracellular matrix (Matrigel, human fibronectin, laminin, and collagen type IV) were observed (data not shown). However, differences in adhesiveness to the stromal cells were obvious. In contrast to the myc-tag and wt D4-GDI clones, the mt D4-GDI clones showed augmented adhesiveness to human bone marrow stromal cells ($p < 0.05$) (Fig. 8). There was a significant difference in adhesion to human stromal cells between the myc-tag clones and the wt D4-GDI clones.

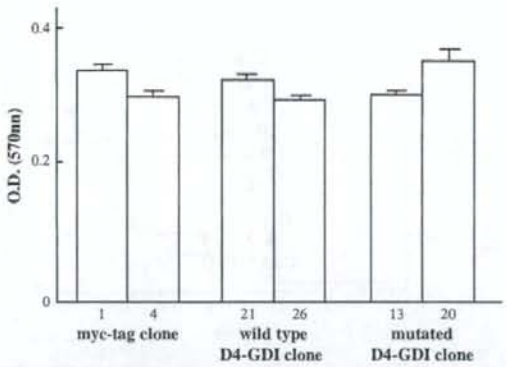

Figure 6. Exogenous D4-GDI expression does not change cell growth rates. The in vitro growth rates of myc-tag clones, wild-type D4-GDI clones, and mutated D4-GDI clones were compared by performing MTT assays. There were no significant differences in proliferative ability among these clones.

Cell-adhesion activity of wt or mt D4-GDI clones (wt3-1, wt3-21, mt13-3, or mt3-27) with a vector of scramble shRNA or a vector for shRNA of Rho-GDI was examined in order to analyze the function of mt D4-GDI under the condition of decreased expression of Rho-GDI. As a result, no differences in adhesion activity between clone wt3-1 and wt3-21, or between clone mt13-3 and mt3-27, were revealed (data not shown).

Detection of cellular GTP-bound Rho, Cdc42, and Rac in leukemic cells

We investigated whether D4-GDI (wt or mt) overexpression in leukemic cells altered Rho and Rac activity. We employed a pull-down assay using RBD affinity-precipitation and Western blotting with anti-RhoA antibody (see Materials and Methods). The proportions of activated Rho (GTP-bound Rho/total Rho) did not differ among myc-tag, wt D4-GDI, and mt D4-GDI clones (Fig. 9). GTP-bound Rho accounted for 1.3% to 1.6 % of total Rho in all experiments. In order to confirm the absence of differences in Rho activity among these clones, the immunoprecipitation with anti-RhoA antibody was carried out after metabolic pulse chase labeling with [^{35}S]-GTPγs. The uptakes of [^{35}S]-GTPγs into RhoA for 8 hours in myc-tag, wt D4-GDI, and mt D4-GDI clones were not different (data not shown). Furthermore, no differences of the

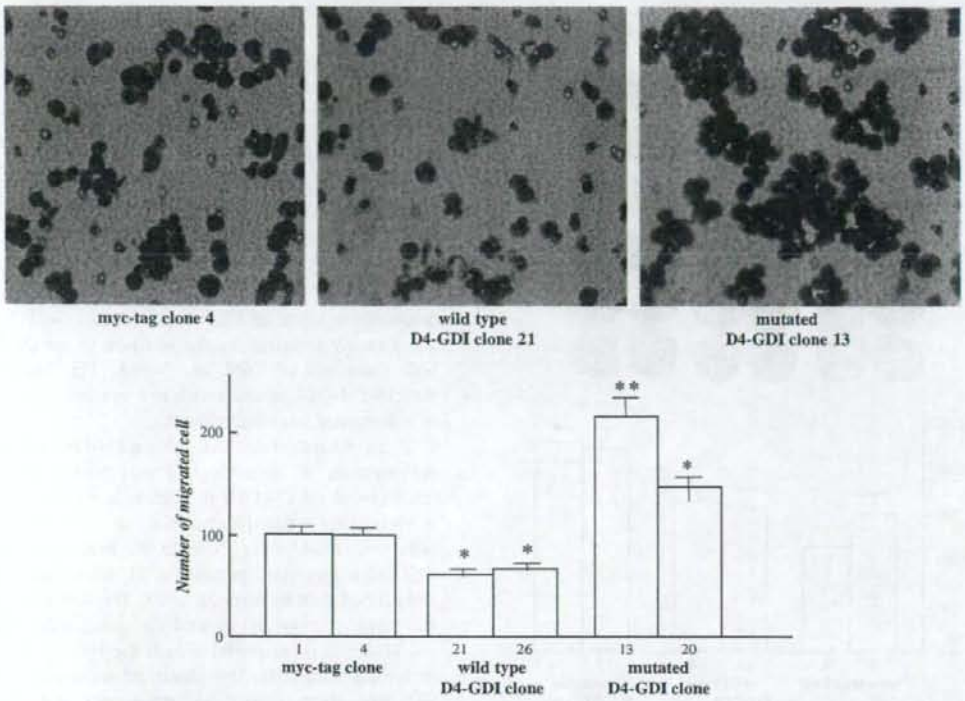

Figure 7. Alteration of cell motility by wild-type or mutated D4-GDI overexpression. The in vitro cellular motile activities of myc-tag clones, wild-type D4-GDI clones, and mutated D4-GDI clones were compared using a chemotaxis chamber (NueroProbe), without hemotactic factors (see Materials and Methods). In contrast to myc-tag clones 1 and 4, mutated D4-GDI clones 13 and 20 showed markedly increased motilities. On the other hand, wild-type D4-GDI clones 21 and 26 showed significantly decreased cell motilities. The upper colored figures show results representative of migrated leukemic cells stained with Diff-Quik (NeuroProbe). Data are represented as mean values. Error bars show standard error of mean. ** and * indicate statistically significant increases ($p < 0.001$ and $p < 0.01$, respectively) as compared to data from myc-tag clone 1 or 4.

Cdc42 and Rac activities between these clones were also observed (Fig. 9A).

Alterations of cellular GTP bound-Rho under the condition of decreased expression of Rho-GDI in leukemic cells with wt D4-GDI or mt D4-GDI overexpression were examined. The pull-down assay for Rho using the wt or mt D4-GDI clones (wt3-1, wt3-21, mt13-3, or mt3-27) with a vector of scramble shRNA or a vector for shRNA of Rho-GDI were done. As a result, the GTP-bound Rho in Rho-GDI knockdown clones (both wt3-21 and mt13-27) was slightly increased compared with clones with scramble shRNA vector (wt3-1 and mt13-3). Especially the difference of GTP-bound Rho/total Rho ratio between mt13-3 and mt13-27 was greater than the difference between wt3-1 and wt3-21. This dissimilarity between wt D4 clones and mt D4 clones in Rho activation by Rho-GDI knockdown may show that the mt D4-GDI proteins impair certain D4-GDI functions.

These results show the exogenous mt D4-GDI expression to be involved in the invasiveness of human leukemic cells through augmentation of cell motility and/or cell-adhesion activity. The altered phenotypes of leukemic cells may be caused by Rho activation due to the mt D4-GDI expression.

Mutated D4-GDI functioned in a dominant negative manner in the inhibition of GDP dissociation from Rho in vitro

While human D4-GDI has been previously shown to inhibit GDP dissociation from Rho family GTPases, we used purified recombinant proteins of wt and mt D4-GDI (V68L or V69A or both V68L and V69A) to directly compare their activities. Sf9 cell–expressed isoprenylated Rho were preloaded with [^{3}H]GDP, and the ability of wt D4-GDI, mt D4-GDIs, and wt plus mt D4-GDIs to inhibit dissociation of the nucleotide was determined. The dissociation of [^{3}H]GDP from Rho was totally blocked by wt D4-GDI (Fig. 10). The dissociation activity of [^{3}H]GDP from Rho by mt D4-GDI with both mutations of V68L and V69A was significantly low. On the other hand, the dissociation activity of mt D4-GDI with single mutation (V68L or V69A) was mild. Furthermore, inhibition of dissociation of [^{3}H]GDP

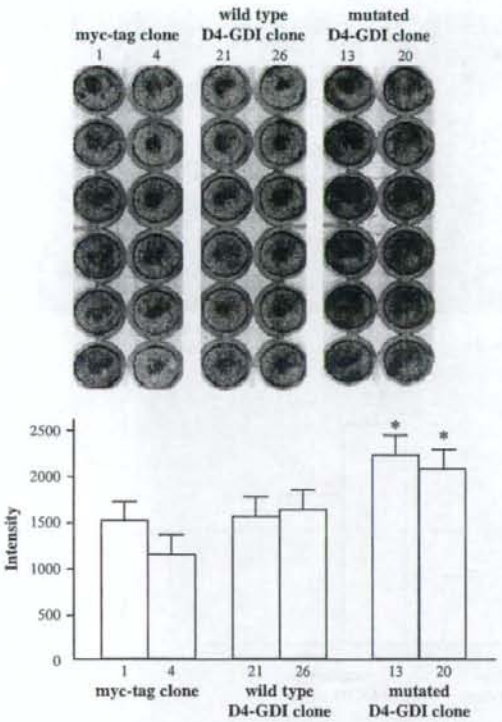

Figure 8. Augmentation of cell adhesion to human bone marrow stromal cells by mutated D4-GDI expression. The cell-adhesion activities of myc-tag clones, wild-type D4-GDI clones, and mutated D4-GDI clones were compared by using quantitative adhesion assays with fluorescent labeling of living cells (see Materials and Methods). In the upper panel, the unlabeled human stromal cells (invisible) attached to all wells and 2,7-bis-(2-carboxyethyl)-5 (and 6) carboxyfluorescein–labeled Raji cell clones, which adhered to the stromal cells were visible like black granules. The vertical line (six wells) represents data derived from one clone. In contrast to myc-tag clones 1 and 4, the mutated D4-GDI clones showed increased adhesiveness to human bone marrow stromal cells ($p < 0.05$). There was no significant difference in adhesion to human stromal cells between the myc-tag clones and wild-type D4-GDI clones. Data are represented as mean values. Error bars show standard error of mean. *Indicates a statistically significant increase ($p < 0.05$) as compared to data from myc-tag clone 1 or 4.

from Rho by wt D4-GDI was impaired by the addition of mt D4-GDI with both mutations of V68L and V69A. The negative effect by the addition of mt D4-GDI with single mutation of V68L orV69A to wt D4-GDI was not observed. As a result, the mt D4-GDI proteins with two mutations may function in a dominant negative manner in vitro.

Discussion

We identified two point mutations of D4-GDI in the human B-cell leukemic cell line. The region of D4-GDI containing these point mutations, which result in amino acid substitutions, is partially conserved in Rho-GDI family genes (Fig. 1). X-ray analysis of the three-dimensional structure of Rho-GDI suggested that these mutations of D4-GDI are in a β-sheet structure [36]. This region is at the back of the continuous surface adjacent to the isoprene-binding site of Rho-GDI, and could easily contact the bound GTPase and impart GDI activity. Robson protein secondary structure prediction suggested that these mutations may influence the β-sheet region [37]. The dissociation activity of GDP of D4-GDI with both mutations of V68L and V69A was decreased greater than the dissociation activity of mt D4-GDI with single mutation (V68L or V69A). Furthermore, dissociation of GDP from Rho by wt D4-GDI was significantly impaired by the addition of mt D4-GDI with both mutations of V68L and V69A. This result suggests that the D4-GDI proteins with two mutations may function in a dominant negative manner.

Thus, we speculated that this mt D4-GDI plays a role in development of hematological malignancy, and analyzed functions of mt D4-GDI in human leukemic cell invasion in vivo using a transplantation model of human leukemic cells into SCID mice. The SCID mice inoculated with Reh cells developed paraplegia 21 days after inoculation and all had died by days 26 to 27. The Reh cells infiltrated into bone marrow and around the spinal cord, with no involvement into peripheral blood, the spleen, liver, thymus or lymph nodes [1]. We identified mutations in the D4-GDI gene from human leukemic cells and showed that overexpression of mt D4-GDI in Raji cells accelerates leukemic cell invasion. Furthermore, we showed that overexpression of wt D4-GDI in Raji cells suppresses invasiveness. Additionally, there were no differences in cell growth rates among these clones, despite the altered invasiveness. On the other hand, cellular motile activity in the mt D4-GDI clones was augmented as compared with the myc-tag clones, and the motile activity of wt D4-GDI clones was significantly decreased. In the cell-adhesion assay, the mt D4-GDI clones showed increased adhesiveness to human bone marrow stromal cells. These findings indicate that the mt D4-GDI functions as a dominant negative molecule against endogenous D4-GDI.

Direct involvement of the Rho family in oncogenesis was discussed in a report [24]. Some GDS with a dbl-homology domain responsible for stimulating nucleotide exchange activity have been reported as potent oncogenes capable of transforming NIH-3T3 cells into a malignant phenotype (e.g., Dbl, Vav, and Lbc) [7,22]. Tiam1 was identified as an invasion-related gene and promoted leukemia progression through activation of the Rac signaling pathway [24]. In contrast to the function of Tiam1 in leukemic cells, Tiam1 and Rac have an invasion-suppressor role in epithelial cells [38]. Rho may also be involved in the increased mobility seen in metastasis through its control of the assembly of focal adhesions [39]. A study suggested that Rho regulates cadherin-mediated adhesion in small